Clinical Pharmacokinetics (2024) 63:919–944
https://doi.org/10.1007/s40262-024-01391-2

REVIEW ARTICLE

Pharmacokinetics–Pharmacodynamics Modeling for Evaluating Drug–Drug Interactions in Polypharmacy: Development and Challenges

Di Zhao[1,2] · Ping Huang[1] · Li Yu[3] · Yu He[1]

Accepted: 3 June 2024 / Published online: 18 June 2024

Abstract

Polypharmacy is commonly employed in clinical settings. The potential risks of drug–drug interactions (DDIs) can compromise efficacy and pose serious health hazards. Integrating pharmacokinetics (PK) and pharmacodynamics (PD) models into DDIs research provides a reliable method for evaluating and optimizing drug regimens. With advancements in our comprehension of both individual drug mechanisms and DDIs, conventional models have begun to evolve towards more detailed and precise directions, especially in terms of the simulation and analysis of physiological mechanisms. Selecting appropriate models is crucial for an accurate assessment of DDIs. This review details the theoretical frameworks and quantitative benchmarks of PK and PD modeling in DDI evaluation, highlighting the establishment of PK/PD modeling against a backdrop of complex DDIs and physiological conditions, and further showcases the potential of quantitative systems pharmacology (QSP) in this field. Furthermore, it explores the current advancements and challenges in DDI evaluation based on models, emphasizing the role of emerging in vitro detection systems, high-throughput screening technologies, and advanced computational resources in improving prediction accuracy.

Key Points

Polypharmacy may lead to DDIs and increases health risks, necessitating a precise assessment.

Summarizing frameworks and quantitation standards of PK and PD models for DDI evaluation aids in refining drug regimens and optimizing dosages.

Advancements in multidisciplinary technologies enhance data and modeling integration, overcome DDI assessment challenges, and advance research.

✉ Yu He
heyu0923@hotmail.com

1 School of Pharmaceutical Sciences, Zhejiang Chinese Medical University, Hangzhou 310000, China

2 Henan University of Chinese Medicine, Zhengzhou, China

3 School of Basic Medical Sciences, Zhejiang Chinese Medical University, Hangzhou, China

1 Introduction

Polypharmacy is a common practice in clinical settings. A National Center for Health Statistics report covering 2015–2018 revealed that 24% of US adults used three or more prescription drugs within a 30-day period, a figure that rises to 66.4% among those aged 65 and older [1, 2]. Given the potential for adverse reactions (ADRs) from drug interactions, the US Food and Drug Administration (FDA) has consistently updated guidelines on drug–drug interactions (DDIs) since 1997 to improve predictions of efficacy and safety in polypharmacy regimens [3, 4].

Drugs undergo a series of processes in the body, including absorption, distribution, metabolism, and excretion (ADME). Pharmacokinetics (PK) studies these processes and their temporal relationships, elucidating the changes in drug concentrations over time. Pharmacodynamics (PD) examines the relationship between drug concentrations at the site of action and the resultant physiological effects, including the timing of these effects. Together, PK and PD determine a drug's efficacy and safety [5, 6]. DDI occurs when one drug (the perpetrator) modifies the in vivo exposure of another drug (the victim), affecting its PK and

PD properties. Potential DDI sites include gastrointestinal absorption, tissue distribution affected by protein binding differences, transporter-mediated transmembrane transport, and enzyme-driven metabolism (Fig. 1) [7, 8]. Extensive mechanistic studies have shown that DDIs can affect PD effects through changes in PK or occur independently at either level. For instance, minor changes in PD effects might lead to overlooking a DDI despite significant PK variations. Conversely, DDIs may alter PD effects without affecting the PK profile, especially when drugs act on different pathways. Identifying and managing DDIs is crucial in both clinical practice and drug development. Researchers utilize quantitative PK and PD models to predict and assess potential DDI risks [9, 10].

PK and PD models serve as a robust framework for assessing DDIs. Empirical PK-based DDI studies typically observe changes in PK parameters of affected drugs. Early studies faced inconsistent assessment standards, but guidance from the FDA and international consensus formation have significantly improved methodologies [11, 12]. The FDA's tiered evaluation strategy categorizes DDI risks based on potential clinical impacts, utilizing empirical base models initially and employing systematic methods and computational tools such as physiologically based pharmacokinetic (PBPK) models for enhanced accuracy if significant DDI potential is identified [13]. In contrast, PD-based DDI research lacks a formal evaluation paradigm from regulatory agencies. Empirical PD models quantify individual drug contributions or overall effects of drugs. Recent shifts towards understanding underlying pathophysiological mechanisms mark significant progress in PD-based DDI modeling [14, 15]. Various factors affecting DDIs have entered the investigation funnel. Technological advancements enable detailed data collection on drug and physiological mechanisms, facilitating the development of sophisticated, physiologically based mathematical models for DDI assessment,

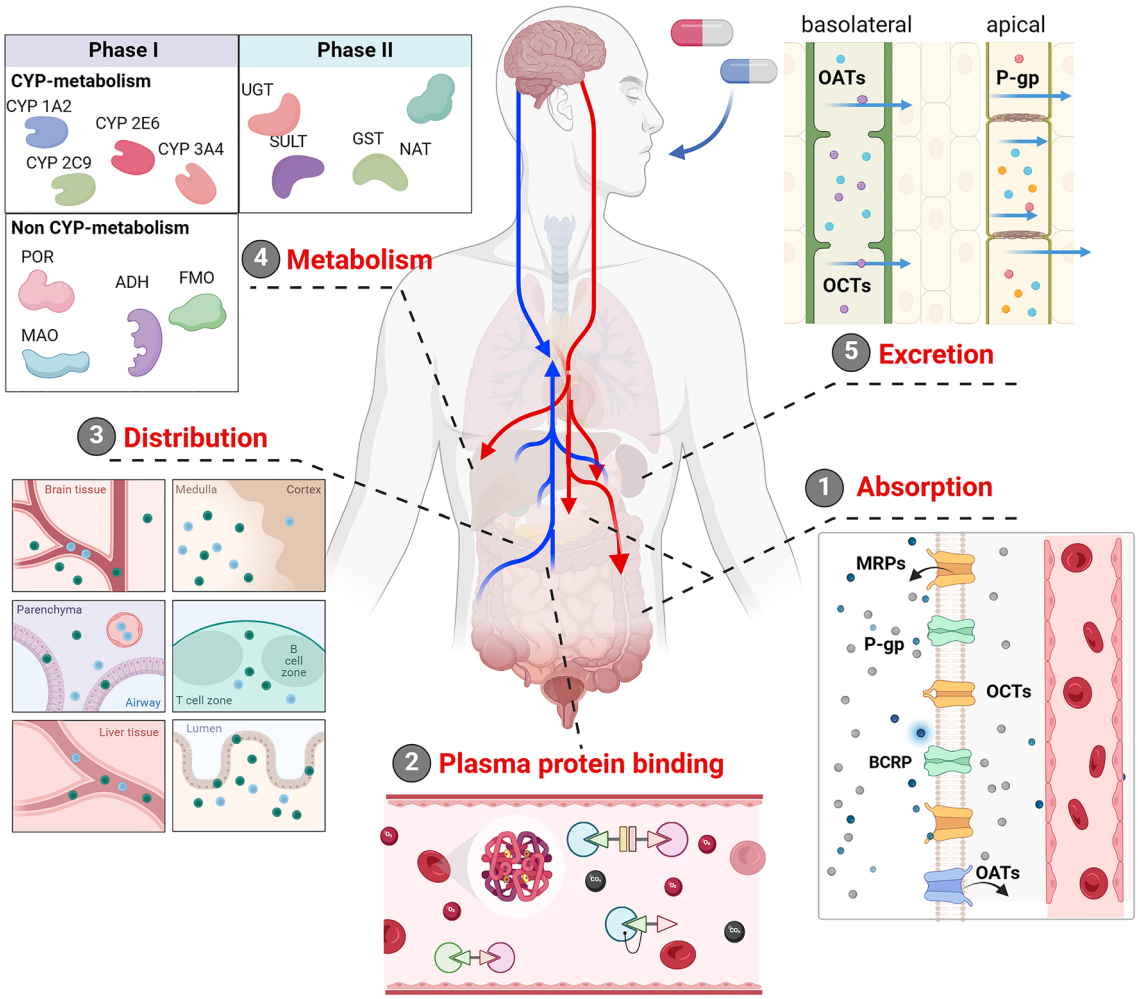

Fig. 1 Determining DDI sites and concentration exposure in vivo is crucial for DDI evaluation. The perpetrator drug may change the victim drug's ADME process by impacting metabolic enzymes and transporters. Key DDI sites are as follows: absorption, plasma protein binding, tissue distribution, metabolism, and excretion

aiding in translating findings from in vitro to in vivo studies and optimizing dosing regimens (Fig. 2) [16].

This review provides a comprehensive analysis of the integration of PK and PD models in the DDI contexts, summarizing traditional empirical models and delving into mechanism-based PK and PD models. This review elaborates on the fundamental theories behind different modeling approaches, emphasizing key threshold values often overlooked in previous reviews for identifying DDI risks. Unlike earlier literature focusing solely on PK or PD aspects, this paper also highlights interrelationship between PK and PD and their practicality in disease treatment [17–19]. Progress and challenges in DDI assessment through PK–PD models are also explored.

2 PK Models for DDIs

The FDA and other regulatory authorities have conducted extensive research and developed guidelines for DDIs mediated by enzymes or transporters using mathematical models. The evaluation begins with conventional static models, which typically rely on the ratio of drug concentrations under steady-state conditions to estimate the effect of one drug on another, without requiring complex dynamic simulations, such as basic models and static mechanism models [20, 21]. Basic models typically employ simplified mathematical equations to describe the interactions within the body. Static mechanism models delve into more detailed considerations of the specific mechanisms of drug interactions, such as enzyme inhibition or induction, and the impact of transport proteins. These models generally evaluate the extent and potential clinical impacts of drug interactions based on mechanistic parameters, such as inhibition constants (*Ki*), maximum induction rates, and others [22, 23]. If static models cannot exclude the risk of DDI, further testing using physiologically based PK (PBPK) models is recommended. PBPK models integrate extensive physiological and biochemical data to simulate the ADME processes of drugs across various tissues and organs, providing a deeper understanding of complex DDI mechanisms [24]. PK-based DDI models are essential quantitative analytical tools for accurately predicting, explaining, and managing DDIs. Table 1 lists the applications of different PK models in DDI risk assessment [25–60].

2.1 Static PK Models

2.1.1 Drug-Metabolizing Enzyme-Mediated DDIs

The area under the plasma drug concentration–time curve (*AUC*) is a critical parameter for evaluating a drug's PK

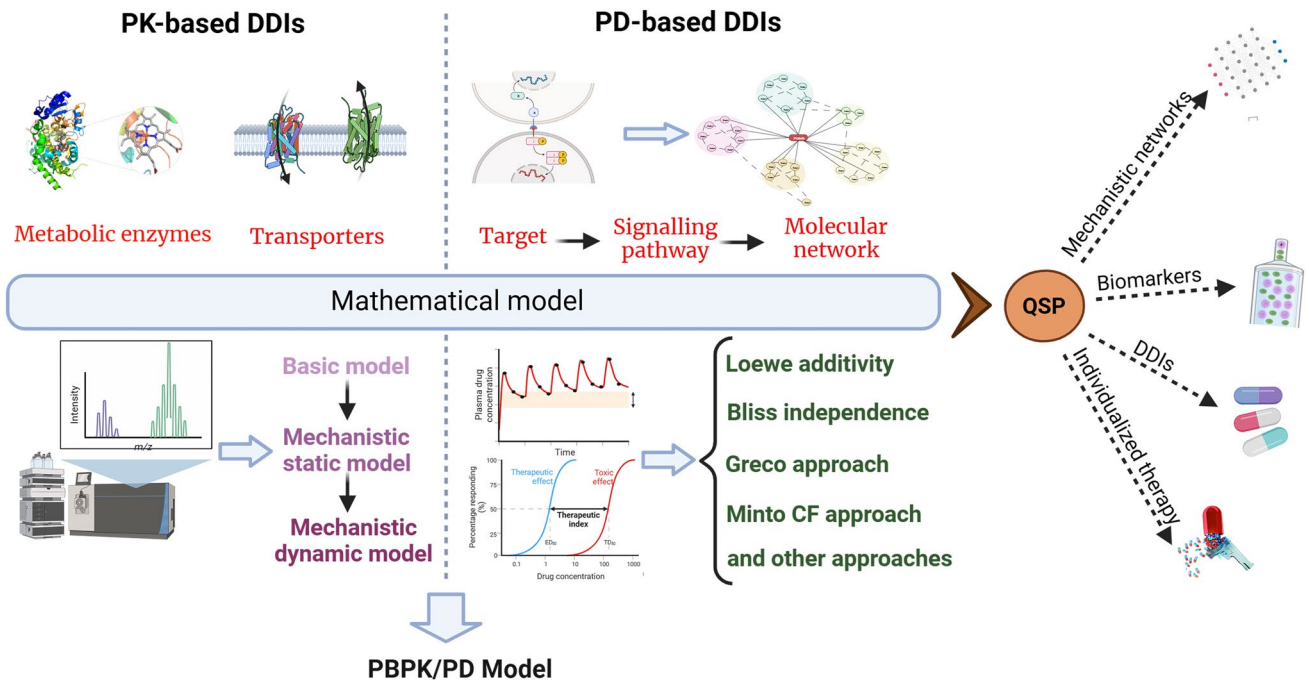

Fig. 2 Various mathematical modeling methods, including empirical, mechanism-based PK/PD, and QSP models, are employed for DDI analysis across experimental systems. Empirical models are typically used in in vitro screenings to assess DDI potential. Mechanism-based models provide a deeper understanding of drug effects, while QSP models explore DDI mechanisms, enhancing insights from the other models

Table 1 Examples of PK models for DDIs

PK models	Victim drug	Perpetrator drug	Underlying mechanism	PK effect	References
Static PK models					
Basic models					
	Ticagrelor	Cyclosporine	(−) CYP3A4	*AUC* ↑	[25]
	Faldaprevir	Efavirenz	(+) CYP3A4	*AUC* ↓, C_{max} ↓, C_{min} ↓	[26]
	Indinavir	Cucurbitacin E	(−) CYP3A4, (−) P-gp	*AUC* ↑, C_{max} ↑. ADR ↑, hepatotoxicity	[27]
	Etoposide	Ketoconazole	(−) P-gp, (−) UGT1A1, (−) CYP3A4	*AUC* ↑, *CL/F* ↓	[28]
	Amlodipine	Efavirenz	(+) CYP3A4	*AUC* ↓	[29]
	Pitavastatin, pravastatin, coproporphyrin-III	Rifampin	(−) OATP1B	*AUC* ↑, C_{max} ↑	[30]
	Furosemide	Novobiocin	(−) BCRP	*AUC* ↑, C_{max} ↑, *CLR* ↓	[31]
	Sulfadiazine, florfenicol	Allicin	(−) P-gp, (−) BCRP	*AUC* ↑, C_{max} ↑, *CLz* ↓	[32]
	Metformin	Olaparib	(−) OCT1, (−) MATE1, (−) MATE2K	*AUC* ↑, C_{max} ↑	[33]
	Carbamazepine	Piperine	(−) CYP3A2	*AUC* ↑, liver microsomal activity↓	[34]
Static mechanism models					
	Rosuvastatin, Atorvastatin,	Darolutamide, letermovir	(−) BCRP, (−) OATP1B1	*AUCR* = 2.62/3.09 > 2, moderate DDI	[35]
	Atorvastatin	Rifampicin	(−) OATP1B1, (−) OATP1B3	*AUCR* = 2~2.2 > 2, moderate DDI	[36]
	Pitavastatin	Rifampin	(−) OATP1B	*AUCR* = 7.55 > 5, strong DDI	[37]
	Rosuvastatin	Atazanavir, lopinavir	(−) BCRP, (−) OATP1B1	Atazanavir: *AUCR* = 2.84 > 2, lopinavir: *AUCR* = 2.16 > 2, moderate DDI	[38]
	Midazolam	Mitragynine	(−) CYP2D6, time-dependent inhibition	*AUCR* = 5.69 > 5, strong DDI. ADR ↑, opioid-like effects	[39]
	Simvastatin acid	Telithromycin	(−) CYP3A4, time-dependent inhibition	*AUCR* = 10.8 > 5, strong DDI	[40]
	Midazolam	Esaxerenone	CYP3A	*AUCR* = 1.80 > 1.25, weak DDI	[41]
	Rivaroxaban	Amiodarone, dronedarone	(−) P-gp	*AUCR* = ~1.37–1.31 > 1.25, weak DDI	[42]
PBPK models					
	Rivaroxaban	Rifampin	(+) CYP 3A4, (+) P-gp	*AUC* ↓, C_{max} ↓, strong DDI	[43]
	Apixaban, rivaroxaban	Enzalutamide	(+) CYP3A4, (+) P-gp	*AUC* ↓, C_{max} ↓, strong DDI	[44]
	Vonoprazan	Efavirenz, rifampin	(+) CYP3A	*AUC* ↓, moderate DDI	[45]
	Saxagliptin	Nicardipine	(−) CYP3A2	*AUC* ↑, Rats: moderate DDI, Human: low DDI risk	[46]
	Phenytoin	Itraconazole	(−) CYP2C9, (−) CYP2C19	*AUC* ↑, weak DDI	[47]
	Cabotegravir, rilpivirine	Rifampicin, rifabutin	(+) UGT1A1, (+) UGT1A9, (+) CYP3A4	*AUC* ↓, Cabotegravir/rilpivirine/rifabutin: weak DDI Cabotegravir/rifampicin, rilpivirine/rifampicin: moderate DDI	[48]
	Venlafaxine	Clarithromycin, Paroxetine	(−) CYP2D6 genetic polymorphism	*AUC* ↑, C_{max} ↑, weak DDI	[49]
	Eliglustat	Ketoconazole, paroxetine	(−) CYP2D6 deficiency	*AUC* ↑, moderate DDI	[50]

Table 1 (continued)

PK models	Victim drug	Perpetrator drug	Underlying mechanism	PK effect	References
	Salbutamol	Fluvoxamine	(−) CYP2C19, (−) CYP2D6, (−) SULTs	*AUC* ↑, weak DDI	[51]
	Zanubrutinib, Acalabrutinib	Voriconazole, Fluconazole, itraconazole	(−) CYP2C19, (−) CYP2C9, (−) CYP3A4	*AUC* ↑, zanubrutinib/triazole: weak DDI, acalabrutinib/triazole: moderate DDI	[52]
	Tacrolimus	Schizandrol B	(−) CYP3A4, (−) CYP3A5	*AUC* ↑, weak DDI	[53]
	Midazolam	Carbamazepine	(+) CYP3A4	*AUC* ↓, weak DDI	[54]
	Oxycodone	Ritonavir	(−) CYP3A4, (−) CYP2D6	*AUC* ↑, C_{max} ↑, weak DDI	[55]
	Tacrolimus	Elexacaftor/tezacaftor/ivacaftor (ETI)	(−) CYP3A4	*AUC* ↑, C_{max} ↑, moderate DDI,	[56]
	Daprodustat	Gemfibrozil	(−) OATP1B, (−) CYP2C8	*AUC* ↑, strong DDI	[57]
	Tegoprazan	Rifampicin	(+) CYP3A4	*AUC* ↓ , C_{max} ↓, moderate DDI	[58]
	Metformin	Cimetidine	(−) OCT1/3	*AUC* ↑, moderate DDI. ADR ↑, lactic acidosis	[59]

AUC area under the curve, C_{max} maximum (peak) plasma drug concentration, *CL* clearance, *ADR* adverse reaction

AUCR Area under the curve ratio. *AUCR* < 1.25, low DDI potential; 1.25 < *AUC* < 2 weak DDI; 2 < *AUCR* < 5 moderate DDI; *AUCR* > 5 strong DDI [60]

profile, indicating its systemic exposure. The evaluation of PK-based DDIs primarily quantifies the impact of DDIs by calculating the victim drug's *AUC* ratio (*AUCR*) in the presence or absence of the perpetrator drug (AUC^i/AUC) [61]. Basic models are predicated on the "well-stirred" assumption, positing that the distribution of a drug within the body is immediately uniform and is eliminated through a single pathway, such as renal excretion or hepatic metabolism. As the simplest PK model, the basic model typically employs first-order linear kinetics to describe the drug elimination process, where the effects of transient plasma binding ($f_{\mu,b}$) and changes in tissue blood flow (Q) are simplified, as shown in Eq. (1) [62, 63].

$$\begin{aligned}\frac{AUC^i_{p.o.}}{AUC_{p.o.}} &= \frac{F^i_h}{F_h} \times \frac{CL_h}{CL^i_h} \\ &= \frac{\frac{Q_H}{Q_H+f_{\mu,b}\times CL^i_{\mu,\mathrm{int}}}}{\frac{Q_H}{Q_H+f_{\mu,b}\times CL_{\mu,\mathrm{int}}}} \times \frac{\frac{Q_H\times f_{\mu,b}\times CL_{\mu,\mathrm{int}}}{Q_H+f_{\mu,b}\times CL_{\mu,\mathrm{int}}}}{\frac{Q_H\times f_{\mu,b}\times CL^i_{\mu,\mathrm{int}}}{Q_H+f_{\mu,b}\times CL^i_{\mu,\mathrm{int}}}} \\ &= \frac{CL_{\mu,\mathrm{int}}}{CL^i_{\mu,\mathrm{int}}}\end{aligned} \tag{1}$$

F represents the bioavailability of the drug, CL denotes the clearance of the drug, and CL_{int} refers to the intrinsic clearance, with AUC^i, F^i, CL^i, and $CL^i{}_{int}$ being the corresponding parameters in the presence of the perpetrator drug. When the Michaelis–Menten equation (Eq. 2) is introduced to describe drug metabolism, it accounts for enzyme saturation effects. Here, V represents the rate of the enzymatic reaction, V_{max} is the maximum rate achieved by the system at saturating substrate concentration, and K_m is the substrate concentration at which the metabolic rate reaches half of V_{max}. Therefore, when the substrate concentration (S) is significantly lower than K_m, the metabolic rate is linearly related to the substrate concentration, simplifying CL_{int} as shown in Eq. (3).

$$V = \frac{V_{\max} \times [S]}{K_{\mathrm{m}} + [S]} \tag{2}$$

$$CL_{\mathrm{int}} = \frac{V}{[S]} = \frac{V_{\max}}{K_{\mathrm{m}}} \tag{3}$$

When a perpetrator drug is introduced, the V_{max} and K_m values of the victim drug are altered. The ratio $CL_{\mu,int}/CL^i{}_{\mu,int}$ is designated as R, representing the fold change in victim exposure resulting from the interaction with the perpetrator drug. R_1, R_2, and R_3 correspond to reversible inhibition, time-dependent inhibition (TDI), and induction, as detailed in Eqs. (4)–(6). $I_{max,u}$ is the maximum unbound plasma concentration of the investigational drug at steady state, whereas $K_{i,u}$ represents the unbound inhibition constant determined through in vitro studies. The observed rate constant for enzyme inactivation is k_{obs}, k_{deg} is the rate constant for enzyme degradation, and k_{inact} is the maximum rate of enzyme inactivation. E_{max} and EC_{50} represent the maximal induction effect and the concentration for half-maximal effect, measured in vitro. Using the cutoff values of R is a common method for predicting the potential for DDIs in basic models. According to the latest FDA DDI guidelines, if $R_1 \geq 1.02$, $R_2 \geq 1.25$, or $R_3 \leq 0.8$, the drug is considered to potentially induce DDIs. Further

investigation is recommended to evaluate the DDI potential using mechanism models [64, 65].

$$R_1 = 1 + \frac{I_{\max,u}}{K_{i,u}} \tag{4}$$

$$\begin{aligned} R_2 &= 1 + \frac{k_{\text{obs}}}{k_{\text{deg}}} \\ &= 1 + \frac{k_{\text{inact}} \times 50 \times I_{\max,u}}{k_{\text{deg}}\left(K_{I,u} + 50 \times I_{\max,u}\right)} \end{aligned} \tag{5}$$

$$R_3 = \frac{1}{1 + \frac{E_{\max} \times 10 \times I_{\max,u}}{EC_{50} + 10 \times I_{\max,u}}} \tag{6}$$

Basic models often rely on simplified assumptions that drug interactions remain static and unchanged throughout the administration period, implying that the effects of the drug are immediate and constant. However, this is obviously inconsistent with most situation. In scenarios where a drug is metabolized through multiple pathways, such as hepatic or intestinal routes, or by different enzymes, it is essential to assess the individual contributions of each pathway or enzyme to the total clearance. Therefore, the modified "Rowland–Maitland" model was proposed, as shown in Eq. (7), where f^i represents the metabolic fraction [66, 67].

$$\begin{aligned} AUCR &= \frac{AUC^i}{AUC} \\ &= \frac{1}{\frac{f^i}{1+\frac{I_u}{K_i}} + (1 - f^i)} \end{aligned} \tag{7}$$

Mechanistic static models enhance prediction accuracy by incorporating additional factors such as enzyme metabolic fractions and unbound liver concentrations, along with more kinetic parameters. They offer a comprehensive substrate disposition process and allow for the quantitative evaluation of the perpetrator drug's impact on the victim drug through various mechanisms. Assuming clearance through both the gut and liver, this is represented in Eq (8).

$$\begin{aligned} R_4 = &\left(\frac{1}{\left(\frac{1}{R_{1,g}} \times \frac{1}{R_{2,g}} \times \frac{1}{R_{3,g}} \right) \times \left(1 - F_g\right) + F_g} \right) \\ &\times \left(\frac{1}{\left(\frac{1}{R_{1,g}} \times \frac{1}{R_{2,g}} \times \frac{1}{R_{3,g}} \right) \times f_{\text{m}} + \left(1 - f_{\text{m}}\right)} \right) \end{aligned} \tag{8}$$

Here, h and g denote hepatic and gastrointestinal (gut) routes, respectively. F_g is the fraction of drug absorbed intestinally but not metabolized, and f_m is the fraction of hepatic substrate clearance mediated by P450s. By integrating Eqs. (4), (5), and (6) into the model, Eq. (9) is derived. If $R_4 < 1.25$ for inhibition or $R_4 > 0.8$ for induction, it indicates the drug's potential to affect metabolic enzyme activity and induce DDI [68].

$$\begin{aligned} R_4 = &\left(\frac{1}{\left(\frac{1}{1+\frac{[I]_g}{K_i}} \times \frac{k_{\text{deg},g}}{k_{\text{deg},g} + \frac{[I]_g \times k_{inact}}{[I]_g + K_I}} \times \left(1 + \frac{E_{\max} \times [I]_g}{[I]_g + EC_{50}}\right) \right) \times \left(1 - F_g\right) + F_g} \right) \\ &\times \left(\frac{1}{\left(\frac{1}{1+\frac{[I]_h}{K_i}} \times \frac{k_{\text{deg},h}}{k_{\text{deg},h} + \frac{[I]_h \times k_{inact}}{[I]_h + K_I}} \times \left(1 + \frac{E_{\max} \times [I]_h}{[I]_h + EC_{50}}\right) \right) \times f_{\text{m}} + \left(1 - f_{\text{m}}\right)} \right) \end{aligned} \tag{9}$$

2.1.2 Transporter-Mediated DDIs

Transporters, such as P-glycoprotein (P-gp), breast cancer resistance proteins (BCRPs), organic anion transporting polypeptides (OATPs), organic cation transporters (OCTs), multidrug and toxin extrusion proteins (MATEs), and organic anion transporters (OATs), play a crucial role in drug bioavailability and systemic clearance by facilitating the transmembrane movement of drugs and their metabolites. Perpetrator drugs can affect the expression and activity of transporters, thereby altering the ADME processes of the victim drug. To evaluate the potential for DDIs, it is essential to assess the transporter's ability to uptake the victim drug, considering its intended site of action and elimination pathways. The assessment process starts with a basic model similar to that used for P450s, generally assuming reversible inhibition and employing IC_{50} or Ki values for evaluation, as represented by Eqs. (10) or (11) [69].

$$R = 1 + \frac{I_{\text{gut}}}{K_i} \tag{10}$$

$$R = 1 + \frac{I_{\max,u}}{IC_{50}} \tag{11}$$

For P-gp or BCRP, transporters crucial for absorption in the small intestine, biliary secretion, and renal secretion, a drug poses a DDI risk for oral administration if $R \geq 11$ (I_{gut} = administered dose/250 mL), and for parenteral administration if $R \geq 1.1$ ($I_{\max,u}$ is the maximum unbound plasma concentration of the drug at steady state). Similarly, for OATs, OCTs, and MATEs, which mainly facilitate renal secretion, $R \geq 1.1$ indicates a potential for DDIs [70].

For OATPs, which are mainly responsible for hepatic or biliary elimination, the threshold for DDI risk is also $R \geq 1.1$, as determined by Eq. (12). In this equation, $f_{u,p}$ denotes the drug's free fraction in plasma, IC_{50} is the median inhibitory

concentration for the unbound drug, and $I_{in,max}$ is the maximum inhibitor concentration in plasma at the entry to the hepatic portal vein [71, 72].

$$R = 1 + \frac{f_{u,p} \times I_{in,\max}}{IC_{50}} \tag{12}$$

Static models are a widely used approach that predicts the potential for DDIs using simplified mathematical equations. These models allow for a quick preliminary evaluation of DDIs and are useful for the initial screening of numerous drugs without the need for complex computations. In the early phases of drug development, both basic and mechanistic static models are crucial for identifying potential DDI risks and informing clinical research design. A study utilizing the DDI static model-assessed polypharmacy strategies, approved from 1998 to 2019, involving antiviral drugs and acid reducers, including proton pump inhibitors, histamine H2 receptor antagonists, and antacids. Clinical research confirmed that 90.5% of cases exhibited trends consistent with the assessment outcomes. The current FDA-proposed model assessment strategy offers significant viable recommendations for managing DDIs associated with high-risk antiviral drugs [73]. However, static models typically do not account for variations in drug concentrations over time within the body, which may lead to inaccuracies in predicting long-term or complex drug interactions. Moreover, their reliance on simplified assumptions may not fully capture the complexities of DDIs, especially those involving multiple metabolic pathways and nonlinear kinetics. To achieve more accurate predictions in such complex scenarios, advanced models such as PBPK models are necessary.

2.2 PBPK Models

PBPK models incorporate a drug's physicochemical properties and biological characteristics, providing significant advantages in assessing complex DDIs. PBPK models are structured with multiple compartments, each representing a different physiological organ (e.g., liver, kidneys, heart), interconnected via the circulatory system to mimic drug transport throughout the body. The model's complexity can be tailored according to the objectives of the research and the data available. The liver, being the primary organ for drug metabolism, is a critical component in these models [74]. PBPK models for DDIs are developed using a bottom-up approach, as illustrated in Fig. 3. Initially, separate models for both perpetrator and victim drugs are constructed, focusing on their distribution and absorption. This involves mathematical representation based on drug properties such as solubility and volume of distribution, and tissue characteristics such as hemodynamics and enzyme expression. Collecting human ADME data, both from in vitro and in vivo studies, is crucial at this stage. This data includes physicochemical properties ($LogP$ and pKa), absorption (P_{eff} and solubility), distribution (B/P, K_p, K_d, $f_{u,p}$), metabolism, and

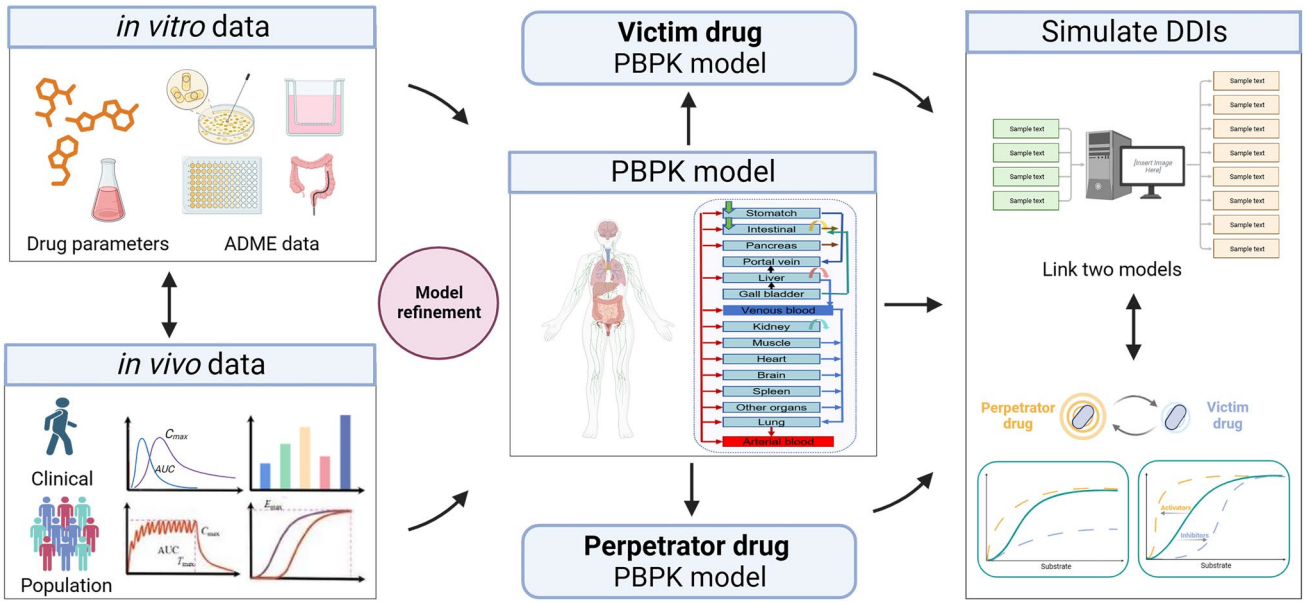

Fig. 3 PBPK models can be utilized to assess DDIs by integrating in vitro experiments and computational predictions of ADME data with human PK data from in vivo studies. The evaluation process involves collecting drug-related data, building and verifying PBPK models of individual drug, simulating interactions between drugs, and analyzing the results to evaluate potential clinical impact. This process requires consideration of factors such as a drug's ADME properties, metabolic pathways, transporter protein competition, etc. to predict PK alterations that may result from DDIs

transport (K_m, V_{max}, J_{max}, CL_{int}), as well as DDI parameters (K_i, K_{inact}, K_I, EC_{50}, and E_{max}). Calibration of these models is achieved by aligning model predictions with observed data to enhance accuracy. Validation then follows, using independent experimental data not previously utilized, often involving PK data from various doses, administration routes, or demographic groups. After validation, the models are linked via equations to predict DDIs, with further validation against in vivo PK data [75, 76].

PBPK models simulate the dynamic distribution and metabolism of drugs within the body, providing time-dependent changes in drug concentration. These models can emulate complex DDIs, including nonlinear effects. Importantly, PBPK models account for physiological and pathological conditions of patients, such as hepatic or renal impairment, age, and weight, which significantly influence drug behavior. They are also applicable to assessing DDIs in special populations like children and pregnant women, who often have limited data in clinical trials [77]. Additionally, PBPK models help reduce costly and time-consuming clinical trials, especially during the early stages of drug development. Establishing a PBPK model requires extensive physiological and drug characteristic data, and the process of building and validating these models is complex [78]. It is an iterative process that benefits from advancements in computing and the growing body of biomedical data. This development necessitates collaboration across disciplines like pharmaceutical science, physiology, biostatistics, and computer science. Currently, platforms such as GastroPlus, SimCyp, PK-Sim, and CLOEPK facilitate the widespread use of PBPK models [18].

3 PD Models for DDIs

A wide range of mathematical modeling approaches have been used to understand PD-based DDIs. The PD models not only assess the risk of DDIs but also evaluate the clinical value of polypharmacy based on the nature of DDIs. Hill's equation is a fundamental basis for describing the dose-response relationship of drugs. Numerous models predict the drug effects based on varying assumptions. The "Interaction–Existence Assumption" model is predicated on the existence of interactions between drugs, implying that the effects of drugs when used together include synergistic and antagonistic actions, exemplified by models like Greco model, the Generalized Drug-Potency Interaction (GPDI) model, Minto model, Chou–Talalay model, and Isobologram analysis exemplify this approach [79–81]. These are nonadditive models. In contrast, the "no interaction assumption" model operates on the premise that drugs act independently, without synergistic or antagonistic interactions, illustrated by models such as the Loewe additivity model and Bliss independence model, falling under additive models [82, 83]. As PD assessment transitions to in vivo studies, models based on physiological mechanisms play a greater role in describing DDI. Table 2 presents examples of the application of PD models in the assessment of DDIs [84–123].

3.1 Conventional PD Models

3.1.1 Nonadditive Model

3.1.1.1 Hill's Equation and Its Variant Models The PD effect of a drug largely depends on its concentration in the body, which can be categorized into central or peripheral compartments. Hill's equation, a cornerstone in modeling dose–response relationships, facilitates the simulation of effects for both single and multiple drug regimens by adjusting its parameters. Specifically, the equation is represented as Eq. (13).

$$E = E_{\max}\frac{D^r}{IC_{50}^r + D^r} \tag{13}$$

$E_{\max}$ is the maximum achievable effect, IC_{50} is the concentration at which 50% of $E_{\max}$ is observed, D is the drug concentration, and r is the Hill coefficient, which describes the steepness of the curve. Notably, when $r = 1$, Hill's equation simplifies to the Michaelis–Menten equation. Hill's equation describes the nonlinear relationship between drug efficacy and concentration, especially when the effect tends to saturate as the concentration increases. It can adjust parameters to reflect the impact of competitive binding to receptors between drugs [124].

Greco and colleagues introduced the universal response surface approach based on the concept of Hill's equation. A key advancement of the Greco model is the introduction of an interaction parameter, α, to quantify DDIs. This parameter allows the model to accurately reflect the primary DDI types—synergism, antagonism, and additivity—and provide a comprehensive description of the dose–effect relationships of drugs, as detailed in Eq. (14). In this model, D_1 and D_2 denote the doses needed to achieve an effect (E) through combined drug administration. The parameter "α" represents the type and degree of DDI. A positive a value indicates a synergistic interaction, while a negative value suggests antagonism. A value of 0 signifies no interaction [125].

$$1 = \frac{d_1}{IC_{50,1}\left(\frac{E}{E_{\max,1}-E}\right)^{1/r_1}} + \frac{d_2}{IC_{50,2}\left(\frac{E}{E_{\max,2}-E}\right)^{1/r_2}} + \frac{ad_1d_2}{IC_{50,1}IC_{50,2}\left(\frac{E}{E_{\max,1}-E}\right)^{1/2r_1}\left(\frac{E}{E_{\max,2}-E}\right)^{1/2r_2}} \tag{14}$$

Table 2 Examples of PD models for DDIs

PD models	Drug 1	Drug 2	Drug 3	Underlying mechanism	PD effect	References
Conventional PD models						
Hill's equation						
	Etomidate	Dexmedetomidine		Additive	Inhibit the secretion of adrenal cortical hormones	[84]
	Ampicillin	Ceftriaxone		Additive	Anti-enterococcal infections	[85]
	Acetaminophen	Ibuprofen	Tramadol	Additive	Prolong analgesia effect	[86]
	Isoniazid	Rifampin		Synergistic or additive	Antibacterial effect	[87]
	Triclabendazole	Amphotericin B		Synergistic	Anti-Leishmania activity	[88]
Greco model						
	Pretomanid	Moxifloxacin		Synergistic	Antituberculosis effect	[89]
	Amphotericin B (AM)	Itraconazole (IT)	Terbinafine (TB)	AM-IT, AM-TB: antagonistic, IT-TB: synergistic	Antifungal effect	[90]
	Moxifloxacin	Pretomanid		Additive	Antituberculosis effect	[91]
	Midazolam	Alfentanil		Synergistic	Sedative and analgesic effect	[92]
	Isavuconazole	Echinocandins			Antifungal effect	[93]
GPDI model						
	Rifampicin	Isoniazid	Ethambutol	Rifampicin/isoniazid: synergistic; rifampicin/ethambutol: synergistic; Rifampicin/isoniazid/ethambutol: Synergistic	Antituberculosis effect	[94]
	Polymyxin B	Minocycline		Synergistic	Antibacterial effect	[95]
	Remifentanil	Propofol		Synergistic	Anesthesia induction and maintenance	[96]
	Docetaxel	SCO-101		Synergistic	Antitumor effect	[97]
	Rifampicin	Isoniazid	Ethambutol	Synergistic	Antituberculosis effect	[98]
Minto model						
	Remifentanil	Propofol		Synergistic	Anesthesia safety	[99]
	Tenofovir, disoproxil, fumarate (TDF)	Emtricitabine (FTC)	Elvitegravir(EVG)	TDF/FTC: synergistic; FTC/EVG: synergistic; TDF/FTC/EVG: antagonistic	Anti-inflammation effect	[100]
	Tetrathiomolybdate	Cisplatin		Synergistic	Antitumor effect	[101]
	Tenuazonic acid	Patulin		Synergistic	Anti-*Caenorhabditis elegans*	[102]
	Alternariol (AOH)	Alternariol monomethyl ether (AME)	Tenuazonic acid (TeA)	AME/AOH: antagonistic; AOH/AME/TeA: synergistic	Toxic effect	[103]
Isobologram analysis						
	Gallic acid	Catechin		Synergistic	Inhibit tyrosinase activity	[104]
	Acrylamide	Fumitremorgin C	Penitrem A	Additive	Antitumor effect	[105]
	Cyanidin-3-*O*-glucoside	Catechin		Synergistic	Inhibit pancreatic lipase activity	[106]
	Remimazolam	Propofol	Sufentanil	Synergistic	Anesthesia induction	[107]

Table 2 (continued)

PD models	Drug 1	Drug 2	Drug 3	Underlying mechanism	PD effect	References
	Besifloxacin	Quercetin		Synergistic	Antibacterial effect	[108]
	Loewe additivity model					
	Glabridin	Voriconazole		Synergistic	Antifungal effect	[109]
	Lovastatin	Tamoxifen, doxorubicin, methotrexate or rapamycin		Synergistic	Antitumor effect	[110]
	Amphotericin B	Colistin		Synergistic	Antifungal effect	[111]
	Clofazimine	Rifampicin	Isoniazid	Synergistic	Antituberculosis effect	[112]
	Loratadine	Desloratadine	Ketoconazole	Additive	Antiarrhythmic effect	[113]
	Bliss independence model					
	5-Fluorouracil	Sertraline	Thioridazine	Synergistic	Antitumor effect	[114]
	LDC4297	Maribavir		Synergistic	Antiviral activity	[115]
	Levofloxacin	Rifabutin	Meropenem	Synergistic	Resistance reduction effect	[116]
	Varoglutamstat	pGlu3-Aβ-specific antibody (m6)		Additive	Anti-alzheimer's disease	[117]
	Obinutuzumab	Bendamustine, doxorubicin, or vincristine		Additive	Antitumor effect	[118]
	Mechanism-based PD models					
	Chicoric acid	Fish oil		Synergistic	Lipid-lowing effect: regulating AMPK-mediated SREBP-1/FAS and PPARα/UCP2 pathways	[119]
	Axitinib	Dabrafenib	PLX4720	Additive	Antitumor effect: upregulating the c-JUN signaling pathway	[120]
	Triptolide	Cinobufagin	Paclitaxel	Synergistic	Antitumor effect: reduces RhoA/ROCK and CDC42/MRCK dual signaling pathways	[121]
	Epigallocatechin-3-*O*-gallate	Fustin		Synergistic	Antitumor effect: activate the eNOS/cGMP axis	[122]
	Sorafenib	Camptothecin		Synergistic	Resistance reduction effect: inhibit the p62-Keap1-Nrf2 pathway enhances iron-induced cell death sensitivity	[123]

Whica and his team introduced the Generalized Drug-Potency Interaction (GPDI) model. The GPDI model essentially expands on Hill's equation by using the sum (or another form of combination) of multiple drug concentrations as a new "effective concentration" and is regarded as semi-mechanistic sometimes [126]. This approach allows the model to assess the overall efficacy of multiple drugs when used together. A common form of the GPDI model is as Eq. (15):

$$E = E_{\max}\frac{\left(\sum_{i=1}^{k} C_i\right)^n}{EC_{50}^n + \left(\sum_{i=1}^{k} C_i\right)^n} \tag{15}$$

C_i represents the concentration of the ith drug. k denotes the total number of drugs. This model classifies drugs as either victims, perpetrators, or both. It assesses the combined effects of drugs by measuring deviations in $E_{\max}$ or EC_{50}, which refer to the drug's effects at concentration C. These deviations are quantified by *INT*, the maximum PD parameter change fraction due to polypharmacy. For drugs with competitive interactions, the GPDI model is compatible with the common additivity model, represented by Eq. (16).

$$1 = \frac{C_1}{EC_{50,1}\times\left(1+\frac{INT_{12}\times C_2^{hINT,12}}{EC50_{INT,12}^{hINT,12}+C_2^{hINT,12}}\right)\times\left(\frac{E_{\text{comb}}}{E_{\max 1}-E_{\text{comb}}}\right)^{1/h_1}} + \frac{C_2}{EC_{50,2}\times\left(1+\frac{INT_{21}\times C_1^{hINT,21}}{EC50_{INT,21}^{hINT,21}+C_1^{hINT,21}}\right)\times\left(\frac{E_{\text{comb}}}{E_{\max 2}-E_{\text{comb}}}\right)^{1/h_2}} \tag{16}$$

INT_{12} quantifies the maximal fractional change in drug1's EC_{50} induced by drug2, while INT_{21} represents the opposite effect. A positive *INT* value signals an EC_{50} increase, a range between −1 and 0 suggests a decrease, and *INT* equal to 0 denotes no interaction. Synergy is inferred when both INT_{12} and INT_{21} are negative, whereas positive values for both indicate antagonism. The variance in *INT* values points to a concentration-dependent relationship, either antagonistic or synergistic. This framework is adept at analyzing DDIs involving two or more drugs, including those with intricate or partially understood mechanisms of action and effect pathways. It enables quantitative assessment of these interactions and handles complex combination data.

Minto et al. developed a model for analyzing PD, which requires that the dose–effect relationship of an individual drug meets Hill's equation. The model is an extension of the classic sigmoid $E_{\max}$ model and characterizes the concentration ratio of drugs by introducing a new variable, θ, that is defined by normalization. The drugs can be seen as a new agent with a fixed combination ratio, θ, that has its own dose–response relationship. The potency of the two drugs is normalized and represented as $U_1 = d_1 / IC_{50,1}$, and $U_2 = d_2/IC_{50,2}$, with the ratio defined as $\theta = U_1/(U_1 + U_2)$. The model's core equation, Eq. (17), calculates the maximum effect [$E_{\max}(\theta)$] of the drug combination at ratio θ. Another critical parameter, $U_{50}(\theta)$, represents the concentration achieving 50% of the maximum effect at this ratio, detailed in Eq. (18) [127].

$$E = E_{\max}(\theta)\frac{\left(\frac{U_1+U_2}{U_{50(\theta)}}\right)^{r(\theta)}}{1+\left(\frac{U_1+U_2}{U_{50(\theta)}}\right)^{r(\theta)}} \tag{17}$$

$$U_{50(\theta)} = \beta_{0,U50} + \beta_{1,U50}\theta + \beta 2_{,U50}\,\theta^2 + \beta_{3,U50}\theta^3 + \beta_{4,U50}\theta^4 \tag{18}$$

The coefficients β_i define model parameters, with $U_{50}(\theta) > 1$ indicating antagonism and $U_{50}(\theta) < 1$ suggesting synergism in PD-based DDIs. This model's ability to quantify drug combination effects has led to its widespread adoption in anesthesia. The Minto model, an evolution of the Greco model, offers enhanced flexibility in analyzing anesthetic agent interactions.

In summary, Hill's equation is fundamental in pharmacology for modeling dose–response curves, providing clear quantification of drug efficacy and potency with parameters such as $E_{\max}$ and EC_{50}. However, it simplifies drug interactions and is less effective for complex, nonmonotonic responses, limiting its direct application in multidrug therapies. The Greco model extends Hill's equation to address synergies and antagonisms in drugs. It offers a more detailed analysis of interactions than Hill's basic model by incorporating effects from multiple drugs, enhancing its utility in DDI assessment. Nonetheless, its reliance on accurate parameter estimation can be challenging in systems with incomplete interaction data. The GDPI model advances the capability to analyze multidrug interactions by integrating the effects of drugs across different pathways and mechanisms. It provides a comprehensive framework for evaluating complex interactions, which is crucial for polypharmacy management. However, the GDPI model requires extensive data to define interactions precisely, which can be a limitation in scenarios with limited experimental data. The Minto model is specifically designed for anesthetic drugs, utilizing PK and PD data to optimize dosing in clinical settings. It excels in predicting the combined effects of anesthetics such as propofol and opioids, aiding in tailored anesthesia management. To accurately quantify PD effects, it is necessary to select appropriate concentration–effect structure models for each drug and use them complementarily to gain a deeper understanding of the mechanisms of PD-based DDI.

3.1.1.2 Chou–Talalay model The Chou–Talalay model, devised by Ting-Chao Chou and Paul Talalay, quantitatively analyzes drugs' effects [128]. The Chou–Talalay model employs the median-effect equation, which is derived from the Michaelis–Menten equation and shares similarities with the Hill equation. However, while the Hill equation is primarily used for dose–response analysis of a single drug, the Chou–Talalay model extends this concept by incorporating a combination index (*CI*) to include the combined effects of multiple drugs, as represented by Eq. (19).

$$f_a = \frac{f_a^m}{1 - f_a^m} = \left(\frac{D}{D_m}\right)^n \tag{19}$$

The f_a represents the fraction of the system affected by the drug, such as the proportion of cells killed or inhibited by the drug. The f^m_a is the level of effect at the median-effect concentration. D is the dose of the drug, while D_m represents the median-effect concentration, similar to EC_{50}. n represents the slope factor, akin to the Hill coefficient in the Hill equation, describing the steepness of the dose–response curve. Adjusting D and D_m allows deriving the median-effect equation for different effect levels. From this analysis, the *CI* can be calculated, presented as Eq. (20) [129].

$$CI = \frac{D_1}{D_{m1}} + \frac{D_2}{D_{m2}} \tag{20}$$

D_1 and D_2 represent the respective doses required for each drug to achieve the effect E when used in combination, while D_{m1} and D_{m2} are the respective doses required for each drug to achieve the same effect E when used individually. The Chou–Talalay model evaluates the interaction between drugs by calculating the *CI*: $CI < 1$ indicates synergy, $CI = 1$ indicates additive effect, and $CI > 1$ indicates antagonism. The Chou–Talalay model provides a quantitative method for assessing DDIs, applicable to various types of drugs and biological effects, such as cytotoxicity, proliferation inhibition, and viral suppression. It is particularly valuable in drug development for cancer treatment, antiviral, and antimicrobial therapies. Moreover, the Chou–Talalay model is adept at managing combinations of drugs at varying doses and proportions, rendering it highly useful for optimizing drug dosages and designing therapeutic strategies. In practice, calculating the *CI*, especially with multiple drugs, can be complex and often requires specialized software such as CompuSyn for accurate *CI* values and effect analysis [130].

3.1.1.3 Isobologram Analysis The isobologram analysis is a graphical method proposed by J. H. Gaddum. This analysis method is based on the equivalence principle, and the type of DDI is judged by comparing the experimentally observed effects with the additive effect expected in theory [131]. First, the effect of each drug is tested independently to determine the dose required to produce a specific effect (such as EC_{50}). Based on the single drug effect, the additive combination dose of two drugs that theoretically produces the same effect is predicted by a mathematical model. The effect of the drug combination is actually tested at different dose ratios to determine the experimental observed combination dose to achieve the same effect level as the single drug. In a two-dimensional coordinate system, the horizontal axis and the vertical axis represent the doses of two drugs respectively. A straight line (additive line) is drawn to connect the dose points of two drugs that produce a specific effect when used alone. Then, the experimental observed drug combination effect points are marked. If the effect points are located on the additive line, the interaction between drugs is additive; if the points are located below the additive line, the interaction between drugs is synergistic; if the points are located above the additive line, the interaction between drugs is antagonistic. Isobologram analysis provides an intuitive and practical tool for understanding and predicting DDIs, especially during the drug screening and optimization phase [132, 133].

Compared with complex mathematical models, Isobologram analysis is easier to understand and interpret, making it suitable for rapid evaluation of DDI potential in pharmaceutical development and clinical trial design. It is applicable to any type of drug combination and is not limited by the mechanisms of drug action. By analyzing the effects at different combination doses, Isobologram can help determine the optimal drug combination dosage, thus optimizing therapeutic effects and reducing adverse reactions. However, Isobologram primarily provides visual analysis results and lacks in-depth quantitative analysis. Moreover, the accuracy of this approach depends on the quality of experimental data and the additive model selected. In practical applications, it may be necessary to combine other models and biological validation to comprehensively evaluate [134, 135].

3.1.2 Additive Models

3.1.2.1 Loewe Additivity Model To evaluate DDIs, the Loewe additivity model, formulated on the premise of "no interaction," serves as a classical approach [136]. This model, especially with its *CI* metric, provides insights into the nature of DDIs at specific inhibition levels, as shown in Eq. (21). The n represents the number of drugs or the number of different effects considered in a model. For a two-drug regimen, the expression is depicted as Eq. (22). The

CI values categorize the interaction as synergistic ($CI < 1$), antagonistic ($CI > 1$), or no interaction ($CI = 1$) based on the doses required to achieve a given effect E, either individually [(D_1) and (D_2)] or in combination [(d_1) and (d_2)].

$$CI = \sum_{i=1}^{n} \frac{d_i}{D_i} \ (n = 1, 2, 3 \ldots \ldots) \tag{21}$$

$$CI = \frac{d1}{D_1} + \frac{d_2}{D_2} \tag{22}$$

The additive model functions as an approximation of the combined treatment effect by representing it as a hypothetical individual response, relying solely on the concentration-effect curve of the drug. This prediction relies on the principle that each drug's dosage contribution to the overall effect is additive. The Loewe additivity model offers a simple and intuitive method for evaluating the effects of drugs, especially in the preliminary research phase. This model operates on the assumption that drugs act independently, allowing the combined dosage-efficacy curve of multiple drugs to be predicted from the individual dosage-efficacy curves of single drugs. However, the Loewe additivity model assumes that the drugs have similar concentration–response curves, a limitation that restricts its predictive capability for diverse therapeutic strategies [137]. To address this, Van der Borght et al. introduced the extended biochemically intuitive generalized Loewe (BIGL) model. This advanced model incorporates a scaling factor, enhancing its flexibility to account for drugs with different maximum effects in the concentration–response relationship [138].

3.1.2.2 Bliss Independence Model Bliss and his associates introduced the Bliss independence model to evaluate the efficacy of drugs using the independence criterion, which notably disregards the nonlinearity of dose–response relationships [139]. This model applies probability theory to deduce the rationality behind combining drugs by calculating the probability (P) of a PD effect occurring, where P ranges between 0 and 1. If the regimen comprises two drugs, the corresponding equations are Eqs. (23) and (24). Specifically, $P(D_1, D_2)$ represents the proportion of the combined effect E to the maximum possible effect E_{max} of the drugs when used in combination, while $P(D)$ indicates the ratio of an individual drug's effect at dose (D) to its maximum effect when administered alone. A measured $P(D_1, D_2)$ value exceeding the model's predicted value suggests synergism, whereas a lower value indicates antagonism [140].

$$P = \frac{E}{E_{\max}} = \frac{\left(\frac{D}{IC_{50}}\right)^r}{1 + \left(\frac{D}{IC_{50}}\right)^r} \tag{23}$$

$$P(D_1, D_2) = P(D_1) + P(D_2) - P(D_1) \cdot P(D_2) \tag{24}$$

The Bliss independence model calculates the combined effect of two drugs by predicting the probability of their independent actions. It is applicable to drugs with different mechanisms, as it does not require the drugs to share the same targets or pathways. This makes the Bliss model particularly useful in multitarget drug research. However, in some cases, the Bliss model may underestimate the true synergistic effects, especially when the mechanisms or pathways of the drugs overlap. The original Bliss independence model often led to false positives due to its failure to consider the variability in drug efficacy [141, 142]. To address this issue, Liu and Zhao et al. [143] developed a two-stage Bliss independence model that evaluates an overall interaction index (τ) with a 95% confidence interval, significantly reducing the risk of false positives. However, as mechanistic assessment methods based on fixed modes of action, both the Loewe additivity model and the Bliss independence model are unable to fully capture the complex DDIs. Meletiadis and Kashif et al. have employed a combined use of these two models to assess polypharmacy strategies in antimicrobial and anticancer therapies. Their validated results have been applied to guide clinical medication regimens [144, 145].

3.2 Mechanism-Based PD Models

Empirical approaches help identify potential combination regimens but face limitations in complex DDI evaluations. Under complex physiological conditions, empirical models that rely on extensive data present challenges and are often unstable in extensive cell line studies. Therefore, PD-based DDI studies require models based on physiological mechanisms to effectively address these challenges [146, 147].

Mechanism-based PD models are founded on a comprehensive understanding of drug action mechanisms. Such models are crucial for evaluating DDIs at the PD level, which typically involve assessing how drugs compete for receptor sites, interfere with signaling pathways, regulate physiological feedback mechanisms, and either augment or negate each other's effects [148, 149]. The initial step involves examining drug–receptor interactions, the cornerstone of PD modeling, which includes analyzing the kinetics of how drugs bind to their specific receptors. Following receptor binding, the focus shifts to signal transduction processes, examining how drugs activate or inhibit intracellular signaling pathways, ultimately leading to pharmacological

outcomes. This phase may encompass a variety of complex mechanisms, including the generation of second messengers and the activation of protein kinases, among others. The final process is the activation (or inhibition) of signaling pathways, leading to specific cellular responses—such as alterations in gene expression, cell differentiation, or apoptosis—that collectively result in the observed pharmacological effects at both the tissue and whole-organism levels [150–152].

Mechanism-based PD models provide profound mechanistic insights and robust predictive capabilities in the study of DDIs, aiding in the optimization of drug dosages and the design of clinical trials, thereby supporting personalized medicine and decision-making assistance. However, these models require extensive interdisciplinary data and involve complex and time-consuming construction and maintenance processes. For instance, in mechanism-based PD models, it is crucial to accurately predict the drug concentrations at target sites. This may require the integration of PD models with PK models to capture the in vivo processes of drugs [153, 154].

4 PK/PD Models for DDIs

PK/PD models are mathematical frameworks in pharmacology designed to describe and predict the interactions between the PK and PD of drugs within the body. These models facilitate understanding the ADME processes of drugs. Quantifying the relationship between drug exposure and response characterizes the impact of DDIs on drug specificity, and physiological and pathological systems [155, 156]. Empirical PK/PD models are typically constructed by assembling the basic PK and PD model components discussed in previous sections. The models focus on establishing relationships between different drug concentrations and drug efficacy using statistical or mathematical methods based on clinical trials or laboratory data, without delving into the specific biological mechanisms behind these relationships. Mechanism-based PK/PD models cover multiple biological parameters and variables to accurately simulate the dynamic processes of drugs in vivo and their interactions. These models pertain to drug site-target distribution, target activation and transduction, and disease progression, as illustrated in Fig. 4 [157, 158]. This multiscale approach allows for the exploration of complex DDIs, accounting for the intricate interplay between various biological components and their dynamic responses to multiple perturbations. Owing to the complexity of biological system, many of the models integrate intricate details of cellular signaling pathways, gene regulatory networks, and physiological processes. The QSP approach is particularly effective in addressing these complex dynamic DDIs.

QSP model offers a detailed biological foundation for the PK/PD model, while the PK/PD model provides quantitative pharmacological data for the QSP model. Together, these models can mutually validate and calibrate each other, forming a closed-loop modeling framework. QSP models have enhanced and expanded the capabilities of mechanistic models by providing a comprehensive view of how various drugs interact within interconnected biological pathway networks [159, 160]. The QSP model integrates diverse data sources such as genomics, proteomics, metabolomics, and physiological data, enabling a mechanistic understanding of drug actions across multiple scales spanning molecular, cellular, tissue, and system levels, as illustrated in Fig. 5 [161]. By bridging the gap between simple target interactions and complex system effects, QSP models enhance the accuracy of DDI predictions and address key challenges in DDI assessment, such as individual response heterogeneity, variability in disease response, stages of disease progression, and optimizing drug therapy while minimizing ADRs [162, 163].

4.1 Drug Site–Target Distribution

The alterations induced by the perpetrator drug on the metabolic attributes of the victim drug at the site of action are primary factors affecting the onset and duration of drug effects. Previous research utilized the "effect compartment model" to describe changes in drug concentration within specific tissues, such as the liver or kidneys, and their PD outcomes [164, 165]. DDI targets include enzyme systems, transporters, receptors, ion channels, and plasma protein binding sites. Drugs acting on the same target can produce synergistic effects in polypharmacy therapy, while those acting on different targets may offer complementary therapeutic benefits. The basis for drug and target binding is the chemical affinity, spatial and charge complementarity, specificity, dynamic adaptability, and influence on target biological activity between the drug molecule and the target. These factors collectively determine a drug's selectivity and efficacy. Some models use receptor theory to elucidate the relationship between the affinity and concentration effects of compounds on receptors. Mehta et al. proposed an integrated model that considers both drug-specific and system-specific characteristics, using human blood–brain barrier (BBB) permeability values derived from animal experiments to successfully predict the concentrations of specific drugs in the human central nervous system (CNS) [166]. Iwasaki et al., utilizing clinical data and human physiological parameters, especially by considering the binding affinity of bortezomib to proteasomes in red blood cells and the proteasome concentration, accurately predicted drug exposure and its target inhibition in the blood based on a mechanistic model. This

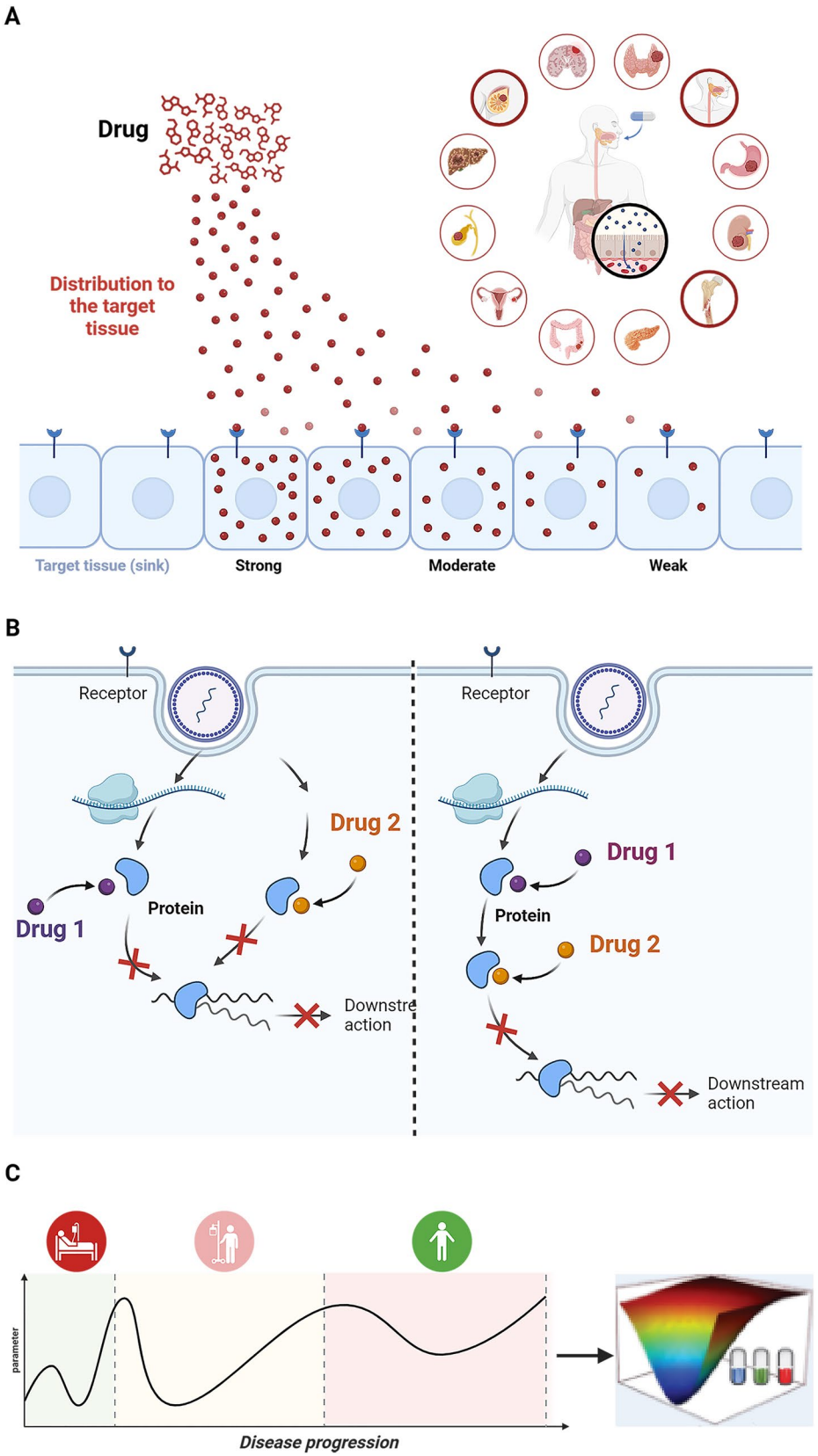

Fig. 4 Mechanistic PK/PD model of DDIs describe the causal relationship between drug exposure and response. **A** Drug target distribution in the circulatory system and tissues is influenced by specificity and adaptability. **B** Factors such as drug–target affinity, receptor expression, and transduction mechanisms affect drug binding to targets and receptor activation. Drugs may act on the same or distinct targets and pathways. **C** Integrating the therapeutic effects into the dynamic changes in disease progression provides personalized and precise guidance for clinical medication use

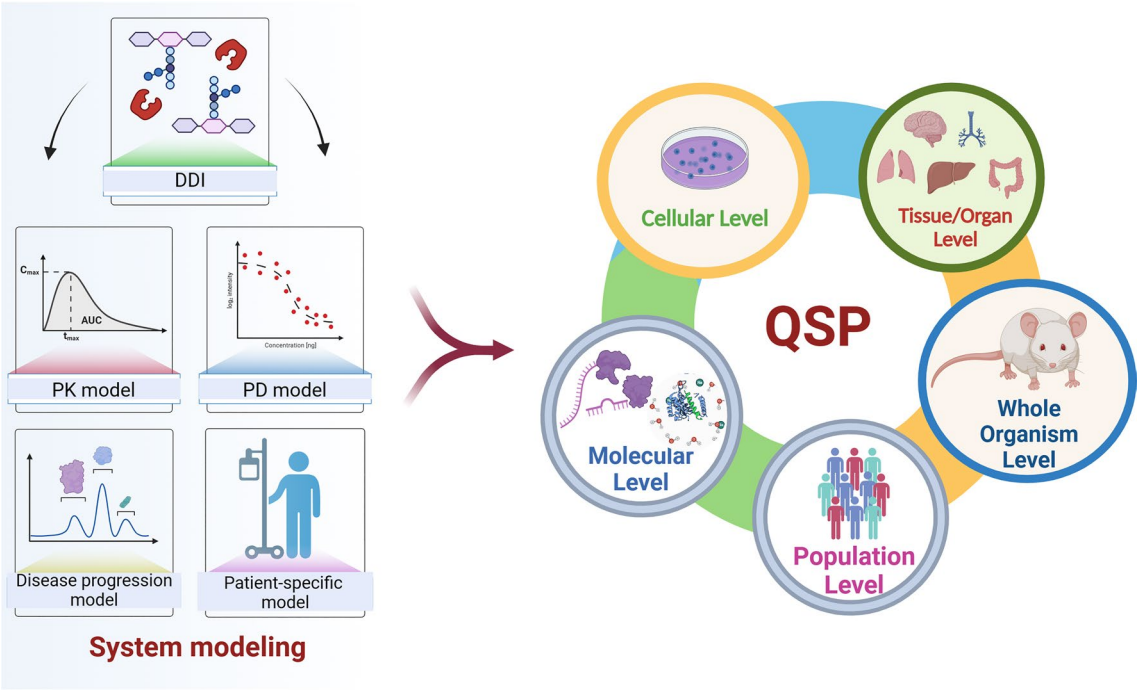

Fig. 5 Polypharmacy is complex, involving a variety of physiological processes across different time frames and locations, including ADME, cellular variability, and whole-organ responses. QSP leverages robust datasets and individual patient characteristics to fine-tune polypharmacy therapy. Moreover, machine learning algorithms provide a robust framework for analyzing large-scale biomedical datasets, predicting pharmacological impacts, refining drug development, and customizing patient care plans

model can also predict the impact of P450 3A inducers and inhibitors on bortezomib exposure, indicating the potential for DDI [167]. Dudas et al. successfully simulated the transitions between the inward and outward states of the transporter ABCG2 and the transport of the endogenous substrate estrone 3-sulfate, providing transition pathways for identifying new substrates and inhibitors as well as exploring drug candidates for DDI [168].

The QSP model provides a dynamic and systematic perspective for understanding of how drugs distribute within the body and interact with biological targets. By integrating PK data with biomarkers and target expression data, QSP models establish relationships between drug concentrations and biological effects. A study employed a QSP model to evaluate the DDI effects of the NK3 receptor (NK3R) antagonist ACER-801 with tamoxifen and leuprolide. This model incorporated the PK, PD, and hepatic metabolism of ACER-801, tamoxifen, and leuprolide. Findings suggested that coadministration of ACER-801 significantly reduces the severity and frequency of vasomotor symptoms in patients treated with tamoxifen or leuprolide, without necessitating adjustments in hormone deprivation therapy due to minimal DDIs [169]. QSP models not only depict the interactions between drugs and their targets and the resultant biological effects but also simulate drug behavior at various dosages and predict the effects of DDIs when multiple drugs are used concurrently.

4.2 Target Activation and Transduction Model

Drug–receptor interactions can either activate or inhibit target functions, impacting both physiological and pathological processes. One factor to consider is the receptor's activation and subsequent signal transduction. This process is the activation of the target to the initiation of the effect, and is characterized by cascading and nonlinear dynamics. DDIs can be regarded as a concentration–effect relationship that is not influenced by time in instances where transduction occurs swiftly and with no discernible metabolic mechanism in the crucial response pathway [170, 171]. Conversely, when transduction within the body is gradual, the manifestation of the effect is intricately linked to time, thereby requiring the adoption of a time-dependent transduction PD model, namely the turnover model. Lint et al. established an integrated two-compartment model describing the PK of carfilzomib incorporating linear disposition. An irreversible deactivation turnover model was built using proteasome activity in peripheral blood mononuclear cells at different times as PD biomarker. By integrating the two models, a mechanism-based PK/PD model with high precision was developed to assess the DDI potential of carfilzomib [172].

In DDI studies, turnover models are frequently employed and examined using various models, including drug metabolizing enzyme kinetic, drug clearance kinetic, drug metabolite kinetic, and drug metabolic pathway regulation models.

By constructing a cascade reversal model, wherein the output of one model serves as the input for another model, it becomes possible to elucidate the biochemical processes involved in drug–target–DDI–biological response interactions. Guo et al. developed an enzymatic turnover model that incorporates both intestinal and hepatic P450 3A induction as well as P-gp effects, aiming to accurately predict P450 3A induction-mediated DDIs. The model initially utilized enzyme kinetics to predict the PK characteristics of 14 P450 3A inducers and substrates. Building on this foundation, it then employed the theory of drug clearance to predict the DDIs between these inducers and substrates. This approach highlighted the significant advantage of turnover model in providing quantitative predictions of DDIs [173]. In PK/PD studies concerning drug–target activation and transduction, QSP models are crucial. These models go beyond merely tracking the relationship between drug concentrations and biological effects. They aim to uncover how drugs trigger complex biological responses by influencing specific biomolecular networks. QSP models provide a comprehensive method for understanding drug mechanisms by simulating and analyzing how drugs affect specific signaling pathways within biological systems. They integrate experimental data related to the target and its signaling pathways, encompassing key parameters such as drug concentrations, target activation states, and changes in signaling molecules [174, 175]. A study applied QSP model to Huntington's disease, utilizing a chemogenomics platform to identify strategies that protect neuronal cells from death induced by mutant huntingtin protein. The research screened several small-molecule probe drugs with distinct mechanisms by measuring phosphorylated PKA levels in the STHdh Q111 cell model. These drugs were found to enhance therapeutic effects and exert synergistic actions by activating the PKA pathway [176]. QSP models are constructed using collected data and should include submodels describing drug PK characteristics (e.g., absorption and clearance mechanisms) and PD submodels (describing drug interactions with targets and subsequent changes in the signaling network) [177, 178].

4.3 Disease Progression Model

Disease progression models (DPMs) encapsulate the dynamic nature of diseases, including changes in disease status and progression rates, which are critical for evaluating DDIs and establishing dosage recommendations [179, 180]. They assess disease progression using diverse data sources, from initial diagnosis to ongoing biomarker data, employing mathematical functions to describe the relationships between biomarkers and disease progression [146, 181]. Key dynamic models, including those for growth, infectious diseases, and tumor growth, can improve predictions of DDIs–disease interactions by being continuously validated with appropriate biomarkers, such as tumor and inflammatory markers. For instance, considering that chronic kidney disease (CKD) affects the clearance rate and distribution volume of drugs, a new virtual severe CKD disease model was developed, incorporating the impact of the disease on both renal and nonrenal pathways, and verified through a PBPK model. The disease model successfully predicted the PK changes of statins in patients with severe CKD and their interaction with Roxadustat, providing guidance for appropriate dosage regimens [182]. DPMs of tumors are used to evaluate the interactions between chemotherapy drugs and other medications (such as painkillers and antibiotics). These models specifically focus on the impact of tumor growth on drug distribution and metabolism, and how adjusting the dosage of chemotherapy drugs can minimize adverse DDIs and optimize treatment outcomes [183]. In the treatment of human immunodeficiency virus/acquired immune deficiency syndrome (HIV/AIDS), DPMs consider the impact of HIV infection on drug metabolic pathways, and how different stages of HIV infection can change the nature and extent of DDIs [184, 185]. QSP models evaluate the potential effects of different drugs on disease progression based on the key biological markers and pathways. Sang et al. developed a translational platform combining human induced pluripotent stem cell-derived cardiomyocytes (hiPSC-CMs) with a QSP–PBPK model to predict systolic dysfunction induced by antineoplastic drugs. This mechanism-based toxicology (TD) model integrates drug exposure, cardiomyocyte interaction, and systemic response, to evaluate DDIs and validate the sequential treatment regimen of amiodarone and trastuzumab [186]. Additionally, the QSP model can simulate how drugs affect inflammatory pathways, cell growth signaling, or apoptosis, enabling longitudinal tracking and prediction of disease progression and therapeutic outcomes. The QSP model integrates tumor-associated macrophages (TAMs), crucial for the immunosuppressive tumor microenvironment, to evaluate the clinical activity of atezolizumab and nab-paclitaxel in triple-negative breast cancer patients with PD-L1-positive, tumor-infiltrating immune cells. This model adeptly captures macrophage heterogeneity and maintains robust predictive accuracy for clinical trials [187].

5 Challenges and Advancements

Advancements in science and technology, such as high-throughput screening tools, advanced in vitro systems, and computational resources, have expanded research into the factors influencing DDIs. These developments have enabled

the collection of detailed data on drug and physiological mechanisms, leading to more sophisticated mathematical models for DDI assessment.

Drug clearance rate is a crucial parameter in the assessment of DDIs. The perpetrator drug can significantly alter the clearance of the victim drug, inducing DDIs. For example, resibufogenin decreases the clearance of amlodipine, leading to an extended half-life and potential adverse reactions [188]. Traditional in vitro systems like human hepatocytes (PHHs) and human liver microsomes (HLMs) are commonly used for in vitro experiments to predict drug clearance. However, these systems have limitations, such as a short survival time of only 4–6 h and a rapid decline in P450 enzyme activity to 10%, making them unsuitable for assessing drugs with low turnover and prolonged half-life [189, 190]. Novel approaches, such as suspension hepatocyte culture techniques, micropatterned cell co-cultures (MPCC), and hepatocyte coculture systems, have shown the ability to maintain liver cell metabolic stability over weeks, offering advantages in predicting low clearance and analyzing metabolite structures [191]. For instance, research teams of Lin and Khetani significantly improved the accuracy of predicting hepatic drug clearance rates in vivo by using MPCCs constructed with cryopreserved non-parenchymal primary human hepatocytes (PHHs) and 3T3-J2 fibroblasts. Compared with traditional PHH suspension and monolayer cultures, MPCCs can maintain function long-term and accurately predict the clearance rates of 26 different drugs with an accuracy ranging from 73% to 96%. By adjusting P450 enzyme activity, it can simulate the impact of drug induction and inhibition on clearance rates, providing an effective tool for predicting drug clearance rates and simulating DDIs [192, 193]. Furthermore, three-dimensional (3D) cell cultures and multiorgan-on-a-chip (MOC) technologies enable detailed exploration of drug pharmacological actions at targeted sites. These methods create a reproducible, controlled microenvironment that simulates in vivo conditions, effectively embodying PBPK models, and have been invaluable in DDI research [194].

As observed in the previous sections on the establishment of PK and PD models, traditional PK/PD research methods typically rely on the average response of tissues or cell populations, ignoring the heterogeneity between cells. The application of single-cell technology in PK/PD model research has provided a new dimension to the study of DDI. By utilizing single-cell mass spectrometry technology, researchers can directly measure drug concentrations within individual cells, providing refined PK information for understanding how drugs distribute across different cell types and subpopulations, as well as their heterogeneity [195]. This approach facilitates a more detailed analysis of the PK properties at the cellular level, enhancing our understanding of drug efficacy and DDI profiles. Through single-cell RNA sequencing (scRNA-seq), researchers can analyze in detail how drugs impact gene expression in different cells, revealing drug-specific effects at the cellular level and mechanisms of drug interactions in complex disease models. This approach allows for a comprehensive understanding of the PD effect within individual cells, providing insights into the efficacy and potential side effects of therapeutic interventions [196, 197]. By collecting single-cell data at different time points, researchers can construct dynamic models of drug interactions, monitoring how drugs influence cell states over time and how drug interactions evolve. Single-cell technology enables data acquisition from individual samples, offering the potential to build personalized PK/PD models that account for inter-individual differences, providing a powerful tool for precision medicine and personalized drug therapy [198].

Research on PK/PD of DDI also faces challenges in establishing accurate exposure–response relationships. On one hand, there is a lack of comprehensive exploration of the mechanisms of individual drugs. Many drugs, such as aspirin and metformin, affect multiple biological pathways and targets through nonspecific actions, leading to complex and variable pharmacological effects, which pose challenges to the quantitative assessment of DDIs [199–201]. On the other hand, the study of DDI mediating factors is insufficient. Non-P450 enzymes, including transport proteins, esterases, aminases, and glucuronosyltransferases, play a crucial role in the ADME processes of drugs. Due to the diversity and wide distribution of these mediating factors, and the significant differences among individuals, the current research on them is relatively inadequate, especially the lack of specific inducers and inhibitors, which increases the difficulty of assessing related DDIs [202]. Omics technologies, including genomics, proteomics, and metabolomics, along with bioinformatics, offer new perspectives for understanding drug mechanisms, pathophysiology, and the potential of DDIs. Omics technologies can identify potential biomarkers that accurately reflect the mechanisms of action and expected activities of drugs, which are crucial for a broad analysis of the molecular composition and function within organisms [203]. Incorporating omics data into PK/PD models can help construct dynamic models that include factors such as gene expression and signal transduction. This integration strengthens DDI research and improves the predictive capability of models, thereby providing more accurate guidance for drug development and clinical application [204].

In accurately modeling complex disease pathways and validating models with large datasets, researchers face significant hurdles in data acquisition and processing. Despite biotechnology advancements enabling vast data collection, the variability in data quality, consistency, and completeness challenges extracting pertinent information and integrating this intricate data effectively. Machine learning

(ML) has become pivotal in discerning patterns within large datasets, enhancing model accuracy and predictive capacity [116]. Specifically, ML excels at identifying correlations between drugs and their physiological impacts. In PK research, it facilitates extracting insights from experimental data, such as predicting metabolic pathways and excretion rates from drug concentration–time curves, crucial for optimizing dosages [205]. It also predicts *AUC* fold changes using FDA drug label information for precise quantitative DDI analysis. Moreover, ML improves drug distribution pattern predictions, aiding in targeted delivery, and broadly predicts DDIs, focusing on P450 enzyme interactions [206, 207]. In PD research, ML is essential for analyzing bioinformatics and genomics data to predict and identify new drug targets, validating their effectiveness by examining target-disease associations [208, 209]. ML identifies complex relationships between PK and PD parameters, guiding model construction [210, 211]. Leveraging big data in PK and PD research not only identifies new targets but also assesses DDI impacts on diverse individuals, broadening research horizons.

6 Conclusion

This article reviews the research models and latest advancements in DDIs based on PK and PD. It highlights how classical basic models and static mechanism models serve as foundational approaches for assessing the potential risks of DDIs from a PK perspective. PBPK models, noted for their dynamic and information-rich capabilities, are increasingly advocated for predicting DDIs more accurately. The PD mathematical model is utilized to evaluate DDIs by comparing the efficacy of single and polypharmacy, aiding in determining whether polypharmacy or specific dosage strategies enhance clinical value. Mechanism-based PK/PD modeling advances this by offering a multiscale, translational research approach that elucidates dose–exposure–response relationships of drugs. QSP models represent a powerful platform for understanding and predicting DDIs by integrating complex biological systems networks. This review underscores the importance of continuously optimizing and integrating experimental resources and computational tools to enhance the accuracy of DDI predictions. In summary, the article serves as a comprehensive reference for updating DDI models and clinical practices, covering various modeling approaches and their applications. The primary objective is to integrate individualized PK and PD characteristics of DDIs, driven and updated by these models, into the regulation and development of clinical medication strategies.

Declarations

Funding This work was supported by the National Natural Science Foundation of China (no. 82374326).

Conflict of Interest Di Zhao, Ping Huang, Li Yu, and Yu He declare that they have no potential conflicts of interest that might be relevant to the contents of this manuscript.

Ethics Approval Not applicable.

Consent to Participate Not applicable.

Consent for Publication Not applicable.

Data Availability All data generated or analyzed during this study are included in this published article (and its supplementary information files).

Code Availability Not applicable.

Author Contributions Di Zhao contributed to the drafting of the manuscript. Yu He obtained funding, designed, conceived, supervised the process, and revised the manuscript. Li Yu and Ping Huang were involved in searching, screening the search results, translation, and data collection and revising the manuscript. All the authors have read and approved the final manuscript.

References

1. Sudsakorn S, Bahadduri P, Fretland J, Lu C. 2020 FDA drug-drug interaction guidance: a comparison analysis and action plan by pharmaceutical industrial scientists. Curr Drug Metab. 2020;21(6):403–26.
2. Krichbaum M, Miransky N, Perez A. Trends in pain medication use in patients with type 2 diabetes: NHANES 2005–2018. J Pain Palliat Care Pharmacother. 2023;37(3):223–33.
3. Hau RK, Wright SH, Cherrington NJ. Addressing the clinical importance of equilibrative nucleoside transporters in drug discovery and development. Clin Pharmacol Ther. 2023;114(4):780–94.
4. Mease J, Ramamoorthy A, Yang X, Madabushi R, Pfuma FE, Zineh I. Statin drug-drug interactions: pharmacokinetic basis of FDA labeling recommendations and comparison across common tertiary clinical resources. J Clin Pharmacol. 2024;64(4):704–12.
5. Su YY, Chiang NJ, Chang JS, Wang YW, Shen BN, Li YJ, et al. The association between UGT1a1 polymorphisms and treatment toxicities of liposomal irinotecan. Esmo Open. 2023;8(1): 100746.
6. Alatwi E, Bairam A. The role of genetic polymorphisms in the sulfation of pregnenolone by human cytosolic sulfotransferase SULT2b1a. Res Sq. 2023; rs.3.rs-3471389.
7. Miao L, Wu F, Yang X, Mousa YM, Ramamoorthy A, Lee S, et al. Application of solubility and dissolution profile comparison for prediction of gastric Ph-mediated drug-drug interactions. AAPS J. 2022;24(1):35–35.
8. Wang CM, Fernez MT, Woolston BM, Carrier RL. Native gastrointestinal mucus: critical features and techniques for studying interactions with drugs, drug carriers, and bacteria. Adv Drug Deliv Rev. 2023;200: 114966.
9. Sun J, Li R, Zhang J, Huang Y, Lu Y, Liu C, et al. Analysis of compatibility mechanism of shenxiong glucose injection after

multiple dosing based on differences of PK-PD correlation and cytochrome P450 enzyme. J Pharm Biomed Anal. 2024;239: 115899.
10. Zhang L, Xie H, Wang Y, Wang H, Hu J, Zhang G. Pharmacodynamic parameters of pharmacokinetic/pharmacodynamic (PK/PD) integration models. Front Vet Sci. 2022;9: 860472.
11. Jang HY, Song J, Kim JH, Lee H, Kim IW, Moon B, et al. Machine learning-based quantitative prediction of drug exposure in drug-drug interactions using drug label information. NPJ Digit Med. 2022;5(1):88.
12. Sall C, Argikar U, Fonseca K, Hilgendorf C, Lopes F, Riedel J, et al. Industry perspective on therapeutic peptide drug-drug interaction assessments during drug development: a European federation of pharmaceutical industries and associations white paper. Clin Pharmacol Ther. 2023;113(6):1199–216.
13. Shan Z, Yang X, Liu H, Yuan Y, Xiao Y, Nan J, et al. Cryo-EM structures of human organic anion transporting polypeptide OATP1b1. Cell Res. 2023;33(12):940–51.
14. Daniel WA, Bromek E, Danek PJ, Haduch A. The mechanisms of interactions of psychotropic drugs with liver and brain cytochrome P450 and their significance for drug effect and drug-drug interactions. Biochem Pharmacol. 2022;199: 115006.
15. Hu W, Zhang W, Zhou Y, Luo Y, Sun X, Xu H, et al. MECDDI: clarified drug–drug interaction mechanism facilitating rational drug use and potential drug–drug interaction prediction. J Chem Inf Model. 2023;63(5):1626–36.
16. Huang L, Chen Q, Lan W. Predicting drug-drug interactions based on multi-view and multichannel attention deep learning. Health Inf Sci Syst. 2023;11(1):50.
17. Wang L, Shendre A, Chiang CW, Cao W, Ning X, Zhang P, et al. A pharmacovigilance study of pharmacokinetic drug interactions using a translational informatics discovery approach. Br J Clin Pharmacol. 2022;88(4):1471–81.
18. Chu X, Prasad B, Neuhoff S, Yoshida K, Leeder JS, Mukherjee D, et al. Clinical implications of altered drug transporter abundance/function and PBPK modeling in specific populations: an ITC perspective. Clin Pharmacol Ther. 2022;112(3):501–26.
19. Shukkoor M, Baharuldin M, Raja K. A text mining protocol for extracting drug-drug interaction and adverse drug reactions specific to patient population, pharmacokinetics, pharmacodynamics, and disease. Methods Mol Biol. 2022;2496:259–82.
20. Colon OR, Knerler S, Fridman LB, Mercado A, Price AS, Rosado-Franco JJ, et al. Cocaine regulates antiretroviral therapy CNS access through pregnane-x receptor-mediated drug transporter and metabolizing enzyme modulation at the blood brain barrier. Fluids Barriers Cns. 2024;21(1):5.
21. Budagaga Y, Sabet Z, Zhang Y, Novotna E, Hanke I, Rozkos T, et al. Tazemetostat synergistically combats multidrug resistance by the unique triple inhibition of ABCB1, ABCC1, and ABCG2 efflux transporters in vitro and ex vivo. Biochem Pharmacol. 2023;216: 115769.
22. Tseng E, Lin J, Strelevitz TJ, Dasilva E, Goosen TC, Obach RS. Projections of drug–drug interactions caused by time-dependent inhibitors of cytochrome P450 1a2, 2b6, 2c8, 2c9, 2c19, and 2d6 using in vitro data in static and dynamic models. Drug Metab Dispos. 2024;52(5):422–31.
23. Gomez-Mantilla JD, Huang F, Peters SA. Can mechanistic static models for drug–drug interactions support regulatory filing for study waivers and label recommendations? Clin Pharmacokinet. 2023;62(3):457–80.
24. Lai Y, Chu X, Di L, Gao W, Guo Y, Liu X, et al. Recent advances in the translation of drug metabolism and pharmacokinetics science for drug discovery and development. Acta Pharm Sin B. 2022;12(6):2751–77.
25. Liu S, Sodhi JK, Benet LZ. Analyzing potential intestinal transporter drug–drug interactions: reevaluating ticagrelor interaction studies. Pharm Res. 2021;38(10):1639–44.
26. Sabo JP, Kort J, Ballow C, Haschke M, Battegay M, Fuhr R, et al. Clinical assessment of potential drug interactions of faldaprevir, a hepatitis c virus protease inhibitor, with darunavir/ritonavir, efavirenz, and tenofovir. Clin Infect Dis. 2014;59(10):1420–8.
27. Lu J, Zhang Y, Sun M, Liu M, Wang X. Comprehensive assessment of cucurbitacin e related hepatotoxicity and drug–drug interactions involving CYP3A and p-glycoprotein. Phytomedicine. 2017;26:1–10.
28. Yong WP, Desai AA, Innocenti F, Ramirez J, Shepard D, Kobayashi K, et al. Pharmacokinetic modulation of oral etoposide by ketoconazole in patients with advanced cancer. Cancer Chemother Pharmacol. 2007;60(6):811–9.
29. Courlet P, Guidi M, Alves SS, Cavassini M, Stoeckle M, Buclin T, et al. Population pharmacokinetic modelling to quantify the magnitude of drug–drug interactions between amlodipine and antiretroviral drugs. Eur J Clin Pharmacol. 2021;77(7):979–87.
30. Bechtold BJ, Lynch KD, Oyanna VO, Call MR, Graf TN, Oberlies NH, et al. Rifampin- and silymarin-mediated pharmacokinetic interactions of exogenous and endogenous substrates in a transgenic OATP1b mouse model. Mol Pharm. 2024;21(5):2284–97.
31. Sharma S, Mettu VS, Prasad B. Interplay of breast cancer resistance protein (BCRP/ABCG2), sex, and fed state in oral pharmacokinetic variability of furosemide in rats. Pharmaceutics. 2023;15(2):542.
32. Wang X, Wang Y, Fang C, Gong Q, Huang J, Zhang Y, et al. Allicin affects the pharmacokinetics of sulfadiazine and florfenicol by downregulating the expression of jejunum p-GP and BCRP in broilers. Poult Sci. 2022;101(7): 101947.
33. Stanislawiak-Rudowicz J, Karbownik A, Szkutnik-Fiedler D, Otto F, Grabowski T, Wolc A, et al. Bidirectional pharmacokinetic drug interactions between olaparib and metformin. Cancer Chemother Pharmacol. 2024;93(1):79–88.
34. Ren T, Yang M, Xiao M, Zhu J, Xie W, Zuo Z. Time-dependent inhibition of carbamazepine metabolism by piperine in antiepileptic treatment. Life Sci. 2019;218:314–23.
35. Asano S, Kurosaki C, Mori Y, Shigemi R. Quantitative prediction of transporter-mediated drug–drug interactions using the mechanistic static pharmacokinetic (MSPK) model. Drug Metab Pharmacokinet. 2024;54:100531.
36. Mitra P, Kasliwala R, Iboki L, Madari S, Williams Z, Takahashi R, et al. Mechanistic static model based prediction of transporter substrate drug–drug interactions utilizing atorvastatin and rifampicin. Pharm Res. 2023;40(12):3025–42.
37. Chu X, Chan GH, Houle R, Lin M, Yabut J, Fandozzi C. In vitro assessment of transporter mediated perpetrator DDIs for several hepatitis C virus direct-acting antiviral drugs and prediction of DDIs with statins using static models. AAPS J. 2022;24(3):45.
38. Elsby R, Coghlan H, Edgerton J, Hodgson D, Outteridge S, Atkinson H. Mechanistic in vitro studies indicate that the clinical drug–drug interactions between protease inhibitors and rosuvastatin are driven by inhibition of intestinal BCRP and hepatic OATP1b1 with minimal contribution from OATP1b3, NTCP and OAT3. Pharmacol Res Perspect. 2023;11(2): e01060.
39. Tanna RS, Tian DD, Cech NB, Oberlies NH, Rettie AE, Thummel KE, et al. Refined prediction of pharmacokinetic kratom–drug interactions: time-dependent inhibition considerations. J Pharmacol Exp Ther. 2021;376(1):64–73.
40. Elsby R, Hare V, Neal H, Outteridge S, Pearson C, Plant K, et al. Mechanistic in vitro studies indicate that the clinical drug–drug interaction between telithromycin and simvastatin acid is driven

by time-dependent inhibition of CYP3A4 with minimal effect on OATP1b1. Drug Metab Dispos. 2019;47(1):1–8.
41. Yamada M, Ishizuka T, Inoue SI, Rozehnal V, Fischer T, Sugiyama D. Drug–drug interaction risk assessment of esaxerenone as a perpetrator by in vitro studies and static and physiologically based pharmacokinetic models. Drug Metab Dispos. 2020;48(9):769–77.
42. Cheong EJ, Goh JJ, Hong Y, Venkatesan G, Liu Y, Chiu GN, et al. Application of static modeling—in the prediction of in vivo drug–drug interactions between rivaroxaban and antiarrhythmic agents based on in vitro inhibition studies. Drug Metab Dispos. 2017;45(3):260–8.
43. Xu RJ, Ling T, Tang H, Ge WH, Jiang Q. Prediction of rivaroxaban–rifampin interaction after major orthopedic surgery: physiologically based pharmacokinetic modeling and simulation. Front Pharmacol. 2021;12: 706781.
44. Otsuka Y, Poondru S, Bonate PL, Rose RH, Jamei M, Ushigome F, et al. Physiologically-based pharmacokinetic modeling to predict drug–drug interaction of enzalutamide with combined p-GP and CYP3A substrates. J Pharmacokinet Pharmacodyn. 2023;50(5):365–76.
45. Mulford DJ, Ramsden D, Zhang L, Michon I, Leifke E, Smith N, et al. Tiered approach to evaluate the CYP3A victim and perpetrator drug–drug interaction potential for vonoprazan using PBPK modeling and clinical data to inform labeling. CPT Pharmacometrics Syst Pharmacol. 2023;12(4):532–44.
46. Lee JM, Yoon JH, Maeng HJ, Kim YC. Physiologically based pharmacokinetic (PBPK) modeling to predict CYP3A-mediated drug interaction between saxagliptin and nicardipine: bridging rat-to-human extrapolation. Pharmaceutics. 2024;16(2):280.
47. Rodriguez-Vera L, Yin X, Almoslem M, Romahn K, Cicali B, Lukacova V, et al. Comprehensive physiologically based pharmacokinetic model to assess drug–drug interactions of phenytoin. Pharmaceutics. 2023;15(10):2486.
48. Bettonte S, Berton M, Stader F, Battegay M, Marzolini C. Management of drug–drug interactions between long-acting cabotegravir and rilpivirine and comedications with inducing properties: a modeling study. Clin Infect Dis. 2023;76(7):1225–36.
49. Cho CK, Kang P, Jang CG, Lee SY, Lee YJ, Bae JW, et al. PBPK modeling to predict the pharmacokinetics of venlafaxine and its active metabolite in different CYP2D6 genotypes and drug–drug interactions with clarithromycin and paroxetine. Arch Pharm Res. 2024. https://doi.org/10.1007/s12272-024-01495-0.
50. Sahasrabudhe SA, Cheng S, Al-Kofahi M, Jarnes JR, Weinreb NJ, Kartha RV. Physiologically-based pharmacokinetic model development, validation, and application for prediction of eliglustat drug–drug interactions. Clin Pharmacol Ther. 2022;112(6):1254–63.
51. Marques L, Vale N. Prediction of CYP-mediated drug interaction using physiologically based pharmacokinetic modeling: a case study of salbutamol and fluvoxamine. Pharmaceutics. 2023;15(6):1586.
52. Chen L, Li C, Bai H, Li L, Chen W. Use of modeling and simulation to predict the influence of triazole antifungal agents on the pharmacokinetics of zanubrutinib and acalabrutinib. Front Pharmacol. 2022;13: 960186.
53. He Q, Bu F, Wang Q, Li M, Lin J, Tang Z, et al. Examination of the impact of CYP3A4/5 on drug–drug interaction between schizandrol a/schizandrol b and tacrolimus (FK-506): a physiologically based pharmacokinetic modeling approach. Int J Mol Sci. 2022;23(9):4485.
54. Kanefendt F, Dallmann A, Chen H, Francke K, Liu T, Brase C, et al. Assessment of the CYP3A4 induction potential by carbamazepine: insights from two clinical DDI studies and PBPK modeling. Clin Pharmacol Ther. 2024;115(5):1025–32.
55. Zheng L, Zhang W, Olkkola KT, Dallmann A, Ni L, Zhao Y, et al. Physiologically based pharmacokinetic modeling of ritonavir-oxycodone drug interactions and its implication for dosing strategy. Eur J Pharm Sci. 2024;194: 106697.
56. Hong E, Carmanov E, Shi A, Chung PS, Rao AP, Forrester K, et al. Application of physiologically based pharmacokinetic modeling to predict drug–drug interactions between elexacaftor/tezacaftor/ivacaftor and tacrolimus in lung transplant recipients. Pharmaceutics. 2023;15(5):1438.
57. Bi YA, Jordan S, King-Ahmad A, West MA, Varma M. Mechanistic determinants of daprodustat drug–drug interactions and pharmacokinetics in hepatic dysfunction and chronic kidney disease: significance of OATP1B-CYP2C8 interplay. Clin Pharmacol Ther. 2024;115(6):1336–45.
58. Ngo LT, Lee J, Yun HY, Chae JW. Development of a physiologically based pharmacokinetic model for tegoprazan: application for the prediction of drug–drug interactions with CYP3A4 perpetrators. Pharmaceutics. 2023;15(1):182.
59. Xie W, Li J, Kong C, Luo W, Zheng J, Zhou Y. Metformin-cimetidine drug interaction and risk of lactic acidosis in renal failure: a pharmacovigilance–pharmacokinetic appraisal. Diabetes Care. 2024;47(1):144–50.
60. Yu J, Wang Y, Ragueneau-Majlessi I. Strong pharmacokinetic drug-drug interactions with drugs approved by the US food and drug administration in 2021: mechanisms and clinical implications. Clin Ther. 2022;44(11):1536–44.
61. Ramsden D, Fullenwider CL. Characterization of correction factors to enable assessment of clinical risk from in vitro CYP3A4 induction data and basic drug–drug interaction models. Eur J Drug Metab Pharmacokinet. 2022;47(4):467–82.
62. Giacomini KM, Yee SW, Koleske ML, Zou L, Matsson P, Chen EC, et al. New and emerging research on solute carrier and atp binding cassette transporters in drug discovery and development: outlook from the international transporter consortium. Clin Pharmacol Ther. 2022;112(3):540–61.
63. Sadaf A, Dong M, Pfeiffer A, Latham T, Kalfa T, Vinks AA, et al. A population pharmacokinetic analysis of l-glutamine exposure in patients with sickle cell disease: evaluation of dose and food effects. Clin Pharmacokinet. 2024;63(3):357–65.
64. Vieira ML, Kirby B, Ragueneau-Majlessi I, Galetin A, Chien JY, Einolf HJ, et al. Evaluation of various static in vitro-in vivo extrapolation models for risk assessment of the CYP3A inhibition potential of an investigational drug. Clin Pharmacol Ther. 2014;95(2):189–98.
65. Kenny JR, Ramsden D, Buckley DB, Dallas S, Fung C, Mohutsky M, et al. Considerations from the innovation and quality induction working group in response to drug–drug interaction guidances from regulatory agencies: focus on CYP3A4 mRNA in vitro response thresholds, variability, and clinical relevance. Drug Metab Dispos. 2018;46(9):1285–303.
66. Miyake T, Mochizuki T, Nakagawa T, Nakamura M, Emoto C, Komiyama N, et al. Quantitative prediction of CYP3A-mediated drug–drug interactions by correctly estimating fraction metabolized using human liver chimeric mice. Br J Pharmacol. 2024;181(7):1091–106.
67. Peng Y, Cheng Z, Xie F. Evaluation of pharmacokinetic drug–drug interactions: a review of the mechanisms, in vitro and in silico approaches. Metabolites. 2021;11(2):75.
68. Nozaki Y, Izumi S. Preincubation time-dependent, long-lasting inhibition of drug transporters and impact on the prediction of drug–drug interactions. Drug Metab Dispos. 2023;51(9):1077–88.
69. Jala A, Ponneganti S, Vishnubhatla DS, Bhuvanam G, Mekala PR, Varghese B, et al. Transporter-mediated drug–drug interactions: advancement in models, analytical tools, and regulatory perspective. Drug Metab Rev. 2021;53(3):285–320.

70. Younis IR, Manchandani P, Hassan HE, Qosa H. Trends in FDA transporter-based post-marketing requirements and commitments over the last decade. Clin Pharmacol Ther. 2022;112(3):635–42.
71. Kayesh R, Tambe V, Xu C, Yue W. Differential preincubation effects of nicardipine on OATP1B1- and OATP1B3-mediated transport in the presence and absence of protein: implications in assessing OATP1B1- and OATP1B3-mediated drug–drug interactions. Pharmaceutics. 2023;15(3):1020.
72. Murray M. Mechanisms and clinical significance of pharmacokinetic drug interactions mediated by FDA and EMA-approved hepatitis C direct-acting antiviral agents. Clin Pharmacokinet. 2023;62(10):1365–92.
73. Shugg T, Powell NR, Marroum PJ, Skaar TC, Younis IR. Evaluation of us food and drug administration drug label recommendations for coadministration of antivirals and acid-reducing agents. Clin Pharmacol Ther. 2022;112(5):1088–97.
74. Jin Z, He Q, Zhu X, Zhu M, Wang Y, Wu XA, et al. Application of physiologically based pharmacokinetic modelling for the prediction of drug–drug interactions involving anlotinib as a perpetrator of cytochrome P450 enzymes. Basic Clin Pharmacol Toxicol. 2022;130(5):592–605.
75. Foti RS. Utility of pbpk modeling in predicting and characterizing clinical drug interactions. Drug Metab Dispos. 2024. https://doi.org/10.1124/dmd.123.001384.
76. Jia G, Ren C, Wang H, Fan C. Prediction of drug–drug interactions between roflumilast and cyp3a4/1a2 perpetrators using a physiologically-based pharmacokinetic (PBPK) approach. BMC Pharmacol Toxicol. 2024;25(1):4.
77. Liu XI, Leong R, Burckart GJ, Dallmann A. Physiologically based pharmacokinetic modeling of nilotinib for drug–drug interactions, pediatric patients, and pregnancy and lactation. J Clin Pharmacol. 2024;64(3):323–33.
78. Hsueh CH, Hsu V, Pan Y, Zhao P. Predictive performance of physiologically-based pharmacokinetic models in predicting drug–drug interactions involving enzyme modulation. Clin Pharmacokinet. 2018;57(10):1337–46.
79. Minto CF, Schnider TW, Short TG, Gregg KM, Gentilini A, Shafer SL. Response surface model for anesthetic drug interactions. Anesthesiology. 2000;92(6):1603–16.
80. Greco WR, Park HS, Rustum YM. Application of a new approach for the quantitation of drug synergism to the combination of cis-diamminedichloroplatinum and 1-beta-d-arabinofuranosylcytosine. Cancer Res. 1990;50(17):5318–27.
81. Weinstein JN, Bunow B, Weislow OS, Schinazi RF, Wahl SM, Wahl LM, et al. Synergistic drug combinations in aids therapy. Dipyridamole/3'-azido-3'-deoxythymidine in particular and principles of analysis in general. Ann N Y Acad Sci. 1990;616:367–84.
82. Shapovalova Y, Heskes T, Dijkstra T. Non-parametric synergy modeling of chemical compounds with gaussian processes. BMC Bioinf. 2022;23(1):14.
83. El HB, Mantini G, Li PG, Capula M, Boyd L, Weinstein H, et al. To combine or not combine: drug interactions and tools for their analysis. Reflections from the EORTC-PAMM course on preclinical and early-phase clinical pharmacology. Anticancer Res. 2019;39(7):3303–9.
84. Gu H, Zhang M, Cai M, Liu J. Combined use of etomidate and dexmedetomidine produces an additive effect in inhibiting the secretion of human adrenocortical hormones. Med Sci Monit. 2015;21:3528–35.
85. Jimenez-Toro I, Rodriguez CA, Zuluaga AF, Otalvaro JD, Perez-Madrid H, Vesga O. Pharmacokinetic/pharmacodynamic index linked to in vivo efficacy of the ampicillin–ceftriaxone combination against enterococcus faecalis. Antimicrob Agents Chemother. 2023;67(2): e0096622.
86. Hannam JA, Anderson BJ, Potts A. Acetaminophen, ibuprofen, and tramadol analgesic interactions after adenotonsillectomy. Paediatr Anaesth. 2018;28(10):841–51.
87. Genestet C, Ader F, Pichat C, Lina G, Dumitrescu O, Goutelle S. Assessing the combined antibacterial effect of isoniazid and rifampin on four mycobacterium tuberculosis strains using in vitro experiments and response-surface modeling. Antimicrob Agents Chemother. 2017;62(1):01413–7.
88. Borges BS, Bueno GP, Tomiotto-Pellissier F, Figueiredo FB, Soares Medeiros LC. In vitro anti-leishmania activity of triclabendazole and its synergic effect with amphotericin b. Front Cell Infect Microbiol. 2023;12:1044665.
89. Drusano GL, Kim S, Almoslem M, Schmidt S, D'Argenio DZ, Myrick J, et al. The funnel: a screening technique for identifying optimal two-drug combination chemotherapy regimens. Antimicrob Agents Chemother. 2021;65(2):e02172–220.
90. Te Dorsthorst DT, Verweij PE, Meis JF, Punt NC, Mouton JW. Comparison of fractional inhibitory concentration index with response surface modeling for characterization of in vitro interaction of antifungals against itraconazole-susceptible and -resistant aspergillus fumigatus isolates. Antimicrob Agents Chemother. 2002;46(3):702–7.
91. de Miranda SC, Hajihosseini A, Myrick J, Nole J, Louie A, Schmidt S, et al. Effect of moxifloxacin plus pretomanid against mycobacterium tuberculosis in log phase, acid phase, and nonreplicating-persister phase in an in vitro assay. Antimicrob Agents Chemother. 2018;63(1):e01695-e1718.
92. Liou JY, Tsou MY, Obara S, Yu L, Ting CK. Plasma concentration based response surface model predict better than effect-site concentration based model for wake-up time during gastrointestinal endoscopy sedation. J Formos Med Assoc. 2019;118(1 Pt 2):291–8.
93. Caballero U, Kim S, Eraso E, Quindós G, Vozmediano V, Schmidt S, et al. In vitro synergistic interactions of isavuconazole and echinocandins against *Candida auris*. Antibiotics (Basel). 2021;10(4):355.
94. Clewe O, Wicha SG, de Vogel CP, de Steenwinkel J, Simonsson U. A model-informed preclinical approach for prediction of clinical pharmacodynamic interactions of anti-tb drug combinations. J Antimicrob Chemother. 2018;73(2):437–47.
95. Aranzana-Climent V, Buyck JM, Smani Y, Pachón-Diaz J, Marchand S, Couet W, et al. Semi-mechanistic PK/PD modelling of combined polymyxin b and minocycline against a polymyxin-resistant strain of *Acinetobacter baumannii*. Clin Microbiol Infect. 2020;26(9):1254.e9-1254.e15.
96. Su H, Koomen JV, Eleveld DJ, Struys M, Colin PJ. Pharmacodynamic mechanism-based interaction model for the haemodynamic effects of remifentanil and propofol in healthy volunteers. Br J Anaesth. 2023;131(2):222–33.
97. Nøhr-Nielsen A, Bagger SO, Brünner N, Stenvang J, Lund TM. Pharmacodynamic modelling reveals synergistic interaction between docetaxel and sco-101 in a docetaxel-resistant triple negative breast cancer cell line. Eur J Pharm Sci. 2020;148:105315.
98. Chen C, Wicha SG, de Knegt GJ, Ortega F, Alameda L, Sousa V, et al. Assessing pharmacodynamic interactions in mice using the multistate tuberculosis pharmacometric and general pharmacodynamic interaction models. CPT Pharmacometr Syst Pharmacol. 2017;6(11):787–97.
99. Jiang Z, Liu Y, Zhang X, Ting CK, Wang X, Brewer LM, et al. Response surface model comparison and combinations for remifentanil and propofol in describing response to esophageal instrumentation and adverse respiratory events. J Formos Med Assoc. 2022;121(12):2501–11.

100. Gallay PA, Ramirez CM, Baum MM. Acute antagonism in three-drug combinations for vaginal HIV prevention in humanized mice. Sci Rep. 2023;13(1):4594.
101. Li Y, Fang M, Xu Z, Li X. Tetrathiomolybdate as an old drug in a new use: as a chemotherapeutic sensitizer for non-small cell lung cancer. J Inorg Biochem. 2022;233: 111865.
102. Zhou H, Yang Y, Kang Y, Guo T, Zhou Y, Zhang Y, et al. Synergistic toxicity induced by the co-exposure of tenuazonic acid and patulin in caenorhabditis elegans: daf-16 plays an important regulatory role. Ecotoxicol Environ Saf. 2024;270: 115871.
103. Lin H, Jia B, Wu A. Cytotoxicities of co-occurring alternariol, alternariol monomethyl ether and tenuazonic acid on human gastric epithelial cells. Food Chem Toxicol. 2023;171: 113524.
104. Xiong Y, Kim HK, Özer ÖÇ, van Duijn B, Korthout H, Zi L, et al. Synergistic inhibiting effect of phytochemicals in rheum palmatum on tyrosinase based on metabolomics and isobologram analyses. Molecules. 2023;28(3):944.
105. Bridgeman L, Juan C, Juan-García A, Berrada H. Individual and combined effect of acrylamide, fumitremorgin c and penitrem a on human neuroblastoma sh-sy5y cells. Food Chem Toxicol. 2023;182: 114114.
106. Wang Y, Chen L, Liu H, Xie J, Yin W, Xu Z, et al. Characterization of the synergistic inhibitory effect of cyanidin-3-o-glucoside and catechin on pancreatic lipase. Food Chem. 2023;404(Pt B): 134672.
107. Lyu S, Deng Q, Lin W, Wu X. Randomized controlled trial for anesthesia during gastroscopy: interactions between remimazolam and propofol in combination with sufentanil. Int J Clin Pharm. 2023;45(4):857–63.
108. Al Hagbani T, Rizvi S, Shakil S, Lila A. Nano-formulating besifloxacin and employing quercetin as a synergizer to enhance the potency of besifloxacin against pathogenic bacterial strains: a nano-synergistic approach. Nanomaterials (Basel). 2023;13(14):2083.
109. Nabili M, Aslani N, Shokohi T, Hedayati MT, Hassanmoghadam F, Moazeni M. In vitro interaction between glabridin and voriconazole against aspergillus fumigatus isolates. Rev Iberoam Micol. 2021;38(3):145–7.
110. Khandelwal Gilman KA, Han S, Won YW, Putnam CW. Complex interactions of lovastatin with 10 chemotherapeutic drugs: a rigorous evaluation of synergism and antagonism. BMC Cancer. 2021;21(1):356.
111. Schwarz P, Nikolskiy I, Bidaud AL, Sommer F, Bange G, Dannaoui E. In vitro activity of amphotericin B in combination with colistin against fungi responsible for invasive infections. J Fungi (Basel). 2022;8(2):112.
112. Mashele SA, Steel HC, Matjokotja MT, Rasehlo S, Anderson R, Cholo MC. Assessment of the efficacy of clofazimine alone and in combination with primary agents against mycobacterium tuberculosis in vitro. J Glob Antimicrob Resist. 2022;29:343–52.
113. Wiśniowska B, Lisowski B, Kulig M, Polak S. Drug interaction at herg channel: in vitro assessment of the electrophysiological consequences of drug combinations and comparison against theoretical models. J Appl Toxicol. 2018;38(4):450–8.
114. Duarte D, Cardoso A, Vale N. Synergistic growth inhibition of HT-29 colon and MCF-7 breast cancer cells with simultaneous and sequential combinations of antineoplastics and CNS drugs. Int J Mol Sci. 2021;22(14):7408.
115. Wild M, Kicuntod J, Seyler L, Wangen C, Bertzbach LD, Conradie AM, et al. Combinatorial drug treatments reveal promising anticytomegaloviral profiles for clinically relevant pharmaceutical kinase inhibitors (PKIs). Int J Mol Sci. 2021;22(2):575.
116. Mukherjee D, Wang P, Hooi L, Sandhu V, You K, Blasiak A, et al. Addressing antimicrobial resistance with the identif.ai platform: rapidly optimizing clinically actionable combination therapy regimens against nontuberculous mycobacteria. Theranostics. 2022;12(16):6848–64.
117. Hoffmann T, Rahfeld JU, Schenk M, Ponath F, Makioka K, Hutter-Paier B, et al. Combination of the glutaminyl cyclase inhibitor PQ912 (varoglutamstat) and the murine monoclonal antibody PBD-Co6 (m6) shows additive effects on brain aβ pathology in transgenic mice. Int J Mol Sci. 2021;22(21):11791.
118. Fujimura T, Yamashita-Kashima Y, Kawasaki N, Yoshiura S, Harada N, Yoshimura Y. Obinutuzumab in combination with chemotherapy enhances direct cell death in CD20-positive obinutuzumab-resistant non-hodgkin lymphoma cells. Mol Cancer Ther. 2021;20(6):1133–41.
119. Mohammadi M, Abbasalipourkabir R, Ziamajidi N. Fish oil and chicoric acid combination protects better against palmitate-induced lipid accumulation via regulating AMPk-mediated SREBP-1/FAS and PPARA/UCP2 pathways. Arch Physiol Biochem. 2023;129(1):1–9.
120. Gunda V, Ghosh C, Hu J, Zhang L, Zhang YQ, Shen M, et al. Combination brafv600e inhibition with the multitargeting tyrosine kinase inhibitor axitinib shows additive anticancer activity in BRAFv600e-mutant anaplastic thyroid cancer. Thyroid. 2023;33(10):1201–14.
121. Wu Q, Ma X, Jin Z, Ni R, Pan Y, Yang G. Zhuidu formula suppresses the migratory and invasive properties of triple-negative breast cancer cells via dual signaling pathways of RHOA/ROCK and CDC42/MRCK. J Ethnopharmacol. 2023;315: 116644.
122. Kumazoe M, Fujimura Y, Yoshitomi R, Shimada Y, Tachibana H. Fustin, a flavanonol, synergically potentiates the anticancer effect of green tea catechin epigallocatechin-3-*O*-gallate with activation of the eNOS/cGMP axis. J Agric Food Chem. 2022;70(11):3458–66.
123. Elkateb AS, Nofal S, Ali SA, Atya HB. Camptothecin sensitizes hepatocellular carcinoma cells to sorafenib- induced ferroptosis via suppression of NRF2. Inflammation. 2023;46(4):1493–511.
124. Xu J, Nelson AG, Hondzinski JM. Passive static stretching alters the characteristics of the force–velocity curvature differently for fast and slow muscle groups—a practical application of hill's equation. Hum Mov Sci. 2021;79: 102852.
125. Franco EJ, Drusano GL, Hanrahan KC, Warfield KL, Brown AN. Combination therapy with UV-4b and molnupiravir enhances SARS-cov-2 suppression. Viruses. 2023;15(5):1175.
126. Wicha SG, Chen C, Clewe O, Simonsson USH. A general pharmacodynamic interaction model identifies perpetrators and victims in drug interactions. Nat Commun. 2017;8(1):2129–211.
127. Scherrer V, Lamoureux F, Chaventre C, Thill C, Demailly Z, Selim J, et al. Reliability of the Minto model for target-controlled infusion of remifentanil during cardiac surgery with cardiopulmonary bypass. Br J Anaesth. 2022;129(2):163–71.
128. Ashton JC. Drug combination studies and their synergy quantification using the Chou-Talalay method—letter. Cancer Res. 2015;75(11):2400.
129. Chou TC. Preclinical versus clinical drug combination studies. Leuk Lymphoma. 2008;49(11):2059–80.
130. Salmaggi A, Corno C, Maschio M, Donzelli S, D'Urso A, Perego P, et al. Synergistic effect of perampanel and temozolomide in human glioma cell lines. J Pers Med. 2021;11(5):390.
131. Huang RY, Pei L, Liu Q, Chen S, Dou H, Shu G, et al. Isobologram analysis: a comprehensive review of methodology and current research. Front Pharmacol. 2019;10:1222.
132. Salinas-Restrepo C, Naranjo-Duran AM, Quintana J, Bueno J, Guzman F, Hoyos PL, et al. Short antimicrobial peptide derived from the venom gland transcriptome of pamphobeteus verdolaga increases gentamicin susceptibility of multidrug-resistant *Klebsiella pneumoniae*. Antibiotics (Basel). 2023;13(1):6.

133. Lafi Z, Alshaer W, Gharaibeh L, Alqudah DA, Alquaissi B, Bashaireh B, et al. Synergistic combination of doxorubicin with hydralazine, and disulfiram against MCF-7 breast cancer cell line. PLoS ONE. 2023;18(9): e0291981.
134. Anastasiadi M, Polizzi K, Lambert R. An improved model for the analysis of combined antimicrobials: a replacement for the Chou-Talalay combination index method. J Appl Microbiol. 2018;124(1):97–107.
135. Kifer D, Jaksic D, Segvic KM. Assessing the effect of mycotoxin combinations: which mathematical model is (the most) appropriate? Toxins (Basel). 2020;12(3):153.
136. Lederer S, Dijkstra T, Heskes T. Additive dose response models: explicit formulation and the Loewe additivity consistency condition. Front Pharmacol. 2018;9:31.
137. Thas O, Tourny A, Verbist B, Hawinkel S, Nazarov M, Mutambanengwe K, et al. Statistical detection of synergy: new methods and a comparative study. Pharm Stat. 2022;21(2):345–60.
138. Van der Borght K, Tourny A, Bagdziunas R, Thas O, Nazarov M, Turner H, et al. Bigl: biochemically intuitive generalized Loewe null model for prediction of the expected combined effect compatible with partial agonism and antagonism. Sci Rep. 2017;7(1):17935.
139. Zhao W, Sachsenmeier K, Zhang L, Sult E, Hollingsworth RE, Yang H. A new Bliss independence model to analyze drug combination data. J Biomol Screen. 2014;19(5):817–21.
140. Ronneberg L, Cremaschi A, Hanes R, Enserink JM, Zucknick M. Bayesynergy: flexible bayesian modelling of synergistic interaction effects in in vitro drug combination experiments. Brief Bioinf. 2021;22(6):bbab251.
141. Goldoni M, Johansson C. A mathematical approach to study combined effects of toxicants in vitro: evaluation of the Bliss independence criterion and the Loewe additivity model. Toxicol In Vitro. 2007;21(5):759–69.
142. Demidenko E, Miller TW. Statistical determination of synergy based on Bliss definition of drugs independence. PLoS ONE. 2019;14(11): e0224137.
143. Liu Q, Yin X, Languino LR, Altieri DC. Evaluation of drug combination effect using a Bliss independence dose–response surface model. Stat Biopharm Res. 2018;10(2):112–22.
144. Kashif M, Andersson C, Mansoori S, Larsson R, Nygren P, Gustafsson MG. Bliss and Loewe interaction analyses of clinically relevant drug combinations in human colon cancer cell lines reveal complex patterns of synergy and antagonism. Oncotarget. 2017;8(61):103952–67.
145. Meletiadis J, Andes DR, Lockhart SR, Ghannoum MA, Knapp CC, Ostrosky-Zeichner L, et al. Multicenter collaborative study of the interaction of antifungal combinations against *Candida* spp. By Loewe additivity and Bliss independence-based response surface analysis. J Fungi (Basel). 2022;8(9):967.
146. Witkowski J, Polak S, Rogulski Z, Pawelec D. In vitro/in vivo translation of synergistic combination of MDM2 and MEK inhibitors in melanoma using PBPK/PD modelling: part II. Int J Mol Sci. 2022;23(19):11939.
147. Yang Y, Chen Y, Wang L, Xu S, Fang G, Guo X, et al. PBPK modeling on organs-on-chips: an overview of recent advancements. Front Bioeng Biotechnol. 2022;10: 900481.
148. Mi K, Zhou K, Sun L, Hou Y, Ma W, Xu X, et al. Application of semi-mechanistic pharmacokinetic and pharmacodynamic model in antimicrobial resistance. Pharmaceutics. 2022;14(2):246.
149. Dudal S, Bissantz C, Caruso A, David-Pierson P, Driessen W, Koller E, et al. Translating pharmacology models effectively to predict therapeutic benefit. Drug Discov Today. 2022;27(6):1604–21.
150. Aksoydan B, Durdagi S. Molecular simulations reveal the impact of ramp1 on ligand binding and dynamics of calcitonin gene-related peptide receptor (CGRPR) heterodimer. Comput Biol Med. 2022;141: 105130.
151. Auerbach A. Dynamics of receptor activation by agonists. Biophys J. 2024. https://doi.org/10.1016/j.bpj.2024.01.003.
152. Maldonado H, Leyton L. CSK-mediated signalling by integrins in cancer. Front Cell Dev Biol. 2023;11:1214787.
153. Hanke N, Turk D, Selzer D, Wiebe S, Fernandez E, Stopfer P, et al. A mechanistic, enantioselective, physiologically based pharmacokinetic model of verapamil and norverapamil, built and evaluated for drug–drug interaction studies. Pharmaceutics. 2020;12(6):556.
154. Wang Z, Xiang X, Liu S, Tang Z, Sun H, Parvez M, et al. A physiologically based pharmacokinetic/pharmacodynamic modeling approach for drug–drug interaction evaluation of warfarin enantiomers with sorafenib. Drug Metab Pharmacokinet. 2021;39: 100362.
155. Takeda T, Hao M, Cheng T, Bryant SH, Wang Y. Predicting drug-drug interactions through drug structural similarities and interaction networks incorporating pharmacokinetics and pharmacodynamics knowledge. J Cheminform. 2017;9:16.
156. Zhang Z, Tang W. Drug metabolism in drug discovery and development. Acta Pharm Sin B. 2018;8(5):721–32.
157. D'Souza S, Prema KV, Balaji S, Shah R. Deep learning-based modeling of drug–target interaction prediction incorporating binding site information of proteins. Interdiscip Sci. 2023;15(2):306–15.
158. Tajaldini M, Poorkhani A, Amiriani T, Amiriani A, Javid H, Aref P, et al. Strategy of targeting the tumor microenvironment via inhibition of fibroblast/fibrosis remodeling new era to cancer chemo-immunotherapy resistance. Eur J Pharmacol. 2023;957: 175991.
159. Geerts H, Spiros A, Roberts P, Carr R. Quantitative systems pharmacology as an extension of PK/PD modeling in CNS research and development. J Pharmacokinet Pharmacodyn. 2013;40(3):257–65.
160. Lu D, Yadav R, Holder P, Chiang E, Sanjabi S, Poon V, et al. Complex PK-PD of an engineered IL-15/IL-15Ralpha-Fc fusion protein in cynomolgus monkeys: QSP modeling of lymphocyte dynamics. Eur J Pharm Sci. 2023;186: 106450.
161. Derbalah A, Al-Sallami H, Hasegawa C, Gulati A, Duffull SB. A framework for simplification of quantitative systems pharmacology models in clinical pharmacology. Brit J Clin Pharm. 2022;88:1430–40.
162. Abbiati RA, Wientjes MG, Au JL. Is it time to use modeling of cellular transporter homeostasis to inform drug–drug interaction studies: theoretical considerations. AAPS J. 2021;23(5):102.
163. Rose R, Mitchell E, Van Der Graaf P, Takaichi D, Hosogi J, Geerts H. A quantitative systems pharmacology model for simulating off-time in augmentation trials for parkinson's disease: application to preladenant. J Pharmacokinet Pharmacodyn. 2022;49(6):593–606.
164. Singla S, Block R. Effect compartment model for the evaluation of tolerance to psychological highness following smoking marijuana. J Clin Pharmacol. 2022;62(12):1539–47.
165. Liu X, Wang J, Huang YW. Quantifying the effect of nano-tio(2) on the toxicity of lead on c. Dubia using a two-compartment modeling approach. Chemosphere. 2021;263:127958.
166. Mehta P, Soliman A, Rodriguez-Vera L, Schmidt S, Muniz P, Rodriguez M, et al. Interspecies brain pbpk modeling platform to predict passive transport through the blood–brain barrier and assess target site disposition. Pharmaceutics. 2024;16(2):226.
167. Iwasaki S, Zhu A, Hanley M, Venkatakrishnan K, Xia C. A translational physiologically based pharmacokinetics/pharmacodynamics framework of target-mediated disposition, target inhibition and drug–drug interactions of bortezomib. AAPS J. 2020;22(3):66.

168. Dudas B, Decleves X, Cisternino S, Perahia D, Miteva MA. Abcg2/bcrp transport mechanism revealed through kinetically excited targeted molecular dynamics simulations. Comput Struct Biotechnol J. 2022;20:4195–205.
169. Baillie R, Schelling C, Ridgewell R, Kudrycki K, Chung D, Friedrich C, et al. Modeling shows the NK3R antagonist, ACER-801, reduces treatment-induced vasomotor symptoms. J Clin Oncol. 2021;39:e13013–e13013.
170. Imai T, Hayakawa M, Ohe K. Development of description framework of pharmacodynamics ontology and its application to possible drug–drug interaction reasoning. Stud Health Technol Inf. 2013;192:567–71.
171. Michinaga S, Nagata A, Ogami R, Ogawa Y, Hishinuma S. Differential regulation of histamine H(1) receptor-mediated ERK phosphorylation by G(q) proteins and arrestins. Biochem Pharmacol. 2023;213: 115595.
172. Lin LH, Ghasemi M, Burke SM, Mavis CK, Nichols JR, Torka P, et al. Population pharmacokinetics and pharmacodynamics of carfilzomib in combination with rituximab, ifosfamide, carboplatin, and etoposide in adult patients with relapsed/refractory diffuse large B cell lymphoma. Target Oncol. 2023;18(5):685–95.
173. Guo H, Liu C, Li J, Zhang M, Hu M, Xu P, et al. A mechanistic physiologically based pharmacokinetic-enzyme turnover model involving both intestine and liver to predict CYP3A induction-mediated drug–drug interactions. J Pharm Sci. 2013;102(8):2819–36.
174. Benson N, van der Graaf PH, Peletier LA. Use of mathematics to guide target selection in systems pharmacology; application to receptor tyrosine kinase (RTK) pathways. Eur J Pharm Sci. 2017;109S:S140–8.
175. Franco YL, Ramakrishnan V, Vaidya TR, Mody H, Perez L, Ait-Oudhia S. A quantitative systems pharmacological approach identified activation of jnk signaling pathway as a promising treatment strategy for refractory HER2 positive breast cancer. J Pharmacokinet Pharmacodyn. 2021;48(2):273–93.
176. Pei F, Li H, Henderson MJ, Titus SA, Jadhav A, Simeonov A, et al. Connecting neuronal cell protective pathways and drug combinations in a Huntington's disease model through the application of quantitative systems pharmacology. Sci Rep. 2017;7(1):17803.
177. Pichardo-Almarza C, Diaz-Zuccarini V. From PK/PD to QSP: understanding the dynamic effect of cholesterol-lowering drugs on atherosclerosis progression and stratified medicine. Curr Pharm Des. 2016;22(46):6903–10.
178. Ayyar VS, Jusko WJ. Transitioning from basic toward systems pharmacodynamic models: lessons from corticosteroids. Pharmacol Rev. 2020;72(2):414–38.
179. Li RJ, Ma L, Li F, Li L, Bi Y, Yuan Y, et al. Model-informed approach supporting drug development and regulatory evaluation for rare diseases. J Clin Pharmacol. 2022;62:S27–37.
180. Madabushi R, Seo P, Zhao L, Tegenge M, Zhu H. Review: role of model-informed drug development approaches in the lifecycle of drug development and regulatory decision-making. Pharm Res. 2022;39(8):1669–80.
181. Ni L, Khan AZ, Long A, Gao L, Toms N, Gonzalez-Gugel E, et al. Optimizing the dosing regimen of cetuximab and ramucirumab using the model-informed drug development paradigm. Clin Pharmacol Ther. 2023;114(1):77–87.
182. Dong J, Prieto GL, Huang Y, Tang W, Lundahl A, Elebring M, et al. Understanding statin-roxadustat drug–drug–disease interaction using physiologically-based pharmacokinetic modeling. Clin Pharmacol Ther. 2023;114(4):825–35.
183. Pfab C, Abgaryan A, Danzer B, Mourtada F, Ali W, Gessner A, et al. Ceftazidime and cefepime antagonize 5-fluorouracil's effect in colon cancer cells. BMC Cancer. 2022;22(1):125.
184. Ambrosioni J, Diaz NA, Marzolini C, Dragovic G, Imaz A, Calcagno A, et al. Outcomes of drug interactions between antiretrovirals and co-medications, including over-the-counter drugs: a real-world study. Infect Dis Ther. 2024;13(3):609–17.
185. Perazzolo S, Shen DD, Scott AM, Ho R. Physiologically based pharmacokinetic model validated to enable predictions of multiple drugs in a long-acting drug-combination nano-particles (DCNP): confirmation with 3 HIV drugs, lopinavir, ritonavir, and tenofovir in DCNP products. J Pharm Sci. 2024;113(6):1653–63.
186. Sang L, Zhou Z, Luo S, Zhang Y, Qian H, Zhou Y, et al. An in silico platform to predict cardiotoxicity risk of anti-tumor drug combination with hIPSC-CMS based in vitro study. Pharm Res. 2024;41(2):247–62.
187. Wang H, Zhao C, Santa-Maria CA, Emens LA, Popel AS. Dynamics of tumor-associated macrophages in a quantitative systems pharmacology model of immunotherapy in triple-negative breast cancer. iScience. 2022;25(8):104702.
188. Zhang C, Gao Z, Niu L, Chen X. Effects of triptolide on pharmacokinetics of amlodipine in rats by using lc-ms/ms. Pharm Biol. 2018;56(1):132–7.
189. Savoj S, Esfahani M, Karimi A, Karamali F. Integrated stem cells from apical papilla in a 3D culture system improve human embryonic stem cell derived retinal organoid formation. Life Sci. 2022;291: 120273.
190. Tischler J, Swank Z, Hsiung HA, Vianello S, Lutolf MP, Maerkl SJ. An automated do-it-yourself system for dynamic stem cell and organoid culture in standard multi-well plates. Cell Rep Methods. 2022;2(7): 100244.
191. Shinha K, Nihei W, Ono T, Nakazato R, Kimura H. A pharmacokinetic-pharmacodynamic model based on multi-organ-on-a-chip for drug–drug interaction studies. Biomicrofluidics. 2020;14(4): 044108.
192. Lin C, Shi J, Moore A, Khetani SR. Prediction of drug clearance and drug–drug interactions in microscale cultures of human hepatocytes. Drug Metab Dispos. 2016;44(1):127–36.
193. Lin C, Khetani SR. Micropatterned co-cultures of human hepatocytes and stromal cells for the assessment of drug clearance and drug–drug interactions. Curr Protoc Toxicol. 2017. https://doi.org/10.1002/cptx.23.
194. Lin N, Zhou X, Geng X, Drewell C, Hübner J, Li Z, et al. Repeated dose multi-drug testing using a microfluidic chip-based coculture of human liver and kidney proximal tubules equivalents. Sci Rep. 2020;10(1):8879.
195. Zhang X, Wei X, Wu CX, Men X, Wang J, Bai JJ, et al. Multiplex profiling of biomarker and drug uptake in single cells using microfluidic flow cytometry and mass spectrometry. ACS Nano. 2024;18(8):6612–22.
196. Zhao S, Xie Y, Ding X, Zheng C, Chen J, Zhao N, et al. Exploring the causal relationship between antihypertensive drugs and glioblastoma by combining drug target Mendelian randomization study, EQTL colocalization, and single-cell RNA sequencing. Environ Toxicol. 2024;39(6):3425–33.
197. Chen B, Zou J, Xie L, Cai Y, Li B, Tan W, et al. WNT-inhibitory factor 1-mediated glycolysis protects photoreceptor cells in diabetic retinopathy. J Transl Med. 2024;22(1):245.
198. Xu Q, Jiang S, Kang R, Wang Y, Zhang B, Tian J. Deciphering the molecular pathways underlying dopaminergic neuronal damage in Parkinson's disease associated with SARS-cov-2 infection. Comput Biol Med. 2024;171: 108200.
199. Dai SX, Li WX, Li GH, Huang JF. Proteome-wide prediction of targets for aspirin: new insight into the molecular mechanism of aspirin. PeerJ. 2016;4: e1791.
200. Zareef R, Diab M, Al ST, Makarem A, Younis NK, Bitar F, et al. Aspirin in COVID-19: pros and cons. Front Pharmacol. 2022;13: 849628.

201. Sakata N. The anti-inflammatory effect of metformin: the molecular targets. Genes Cells. 2024;29(3):183–91.
202. Yamamiya I, Hunt A, Takenaka T, Sonnichsen D, Mina M, He Y, et al. Evaluation of the cytochrome P450 3A and p-glycoprotein drug–drug interaction potential of futibatinib. Clin Pharmacol Drug Dev. 2023;12(10):966–78.
203. Zeuner S, Vollmer J, Sigaud R, Oppermann S, Peterziel H, Elharouni D, et al. Combination drug screen identifies synergistic drug interaction of BCL-xl and class I histone deacetylase inhibitors in MYC-amplified medulloblastoma cells. J Neurooncol. 2024;166(1):99–112.
204. Tan S, Willemin ME, Snoeys J, Shen H, Rostami-Hodjegan A, Scotcher D, et al. Development of 4-pyridoxic acid pbpk model to support biomarker-informed evaluation of OAT1/3 inhibition and effect of chronic kidney disease. Clin Pharmacol Ther. 2023;114(6):1243–53.
205. Watanabe R, Kawata T, Ueda S, Shinbo T, Higashimori M, Natsume-Kitatani Y, et al. Prediction of the contribution ratio of a target metabolic enzyme to clearance from chemical structure information. Mol Pharm. 2023;20(1):419–26.
206. Ai N, Fan X, Ekins S. In silico methods for predicting drug-drug interactions with cytochrome P-450s, transporters and beyond. Adv Drug Deliv Rev. 2015;86:46–60.
207. Ai D, Cai H, Wei J, Zhao D, Chen Y, Wang L. Deepcyps: a deep learning platform for enhanced cytochrome P450 activity prediction. Front Pharmacol. 2023;14:1099093.
208. Zhou Y, Chen SJ. Advances in machine-learning approaches to rna-targeted drug design. Artif Intell Chem. 2024;2(1): 100053.
209. Asfand-E-Yar M, Hashir Q, Shah AA, Malik H, Alourani A, Khalil W. Multimodal CNN-DDI: using multimodal CNN for drug to drug interaction associated events. Sci Rep. 2024;14(1):4076.
210. Sun L, Mi K, Hou Y, Hui T, Zhang L, Tao Y, et al. Pharmacokinetic and pharmacodynamic drug–drug interactions: research methods and applications. Metabolites. 2023;13(8):897.
211. Hasselgren C, Oprea TI. Artificial intelligence for drug discovery: are we there yet? Annu Rev Pharmacol Toxicol. 2024;64:527–50.